LOW SPEED WIND TUNNEL INVESTIGATION OF HIGH LIFT DEVICES ON A 65° SWEPT-BACK SUPERSONIC WING OF 3.44 ASPECT RATIO

Thesis by

John W. Thomas

In Partial Fulfillment of the Requirements

For the Degree of

Aeronautical Engineer

California Institute of Technology

Pasadena, California

1949

ACKNOWLEDGEMENTS

The author wishes to express his sincere gratitude to Mr. Henry T. Nagamatsu for his guidance and assistance in the conduct of the experimental work and the preparation of this thesis.

The author further wishes to express his appreciation to Mr. Michael Marx, with whose very able cooperation the experimental work was carried out.

Special thanks are also due to Dr. E. E. Sechler for his help in the design and fabrication of the model, and to Mr. Bartsch and his machine shop staff for their fine workmanship in building the model.

TABLE OF CONTENTS

TABLE OF FIGURES

I. SUMMARY

A low speed investigation was made in the Cal Tech-Merrill Wind Tunnel at Pasadena City College of a 3.44 aspect ratio wing, having a 65° swept-back leading edge and a symmetrical double-wedge airfoil section, to determine the characteristics and effectiveness of various high-lift devices. The investigation included tests of trailing edge split flaps and extended split flaps, leading edge flaps and slats, and combined configurations. The tests were carried out using the wing with and without the fuselage and tail surfaces.

The results showed that the split flaps increased the lift over the lower regions of the angle of attack only. The extended split flaps were more effective and increased the lift over the whole range. The nose flaps tested did not increase the lift when used by themselves, but the combination of a nose flap with the fuselage and extended split flap produced the greatest lift. The addition of the fuselage added to the lift by increasing the slope of the lift curve. The addition of the tail surface gave additional increments in lift in the upper regions of angle of attack. The maximum lift coefficient, $C_{L_{max.}}$, normally occurred at an angle of attack of 38°.

The extended split flaps produced large variations in pitching moment, but had stabilizing tendencies except where there were irregularities in the lift curve.

II. INTRODUCTION

High performance in supersonic flight calls for thin, uncambered wings which, in turn, produce low lift coefficients at low subsonic speeds. This conflict leads to a difficult problem in obtaining safe landing speed for a supersonic airplane. Furthermore, stability and drag considerations seem to call for swept wings, which sometimes lead to undesirable moment characteristics.

Considerable attention has been focused on these problems in recent years, and along this line, a program was initiated to obtain a systematic collection of experimental results determined from low speed tests on various planform configurations. It was under this program that Jensen and Koerner (Cf. Ref. 1) investigated a 65° swept-back wing of fairly low aspect ratio and a Delta wing, both with double-wedge symmetrical airfoil sections. Densmore and Blenkush (Cf. Ref. 2) are concurrently investigating a rectangular wing and the wing of Ref. 1 in a swept-forward condition. It was in the furtherance of obtaining further experimental data under this program that this research was instituted.

The particular phase incorporated in this thesis is the investigation of a wing of higher aspect ratio (twice as high as that of Ref. 1). For purposes of comparison, the same degree of sweep-back, approximately the same root thickness and taper ratio, the same fuselage, and the same wing area were used as were used in Ref. 1. In the further interests of comparison, the same types of high-lift

devices were used, with some additional variations in the hope of obtaining some particularly effective configuration. Therefore, the purpose of this report may be defined as being the determination of the effect of higher aspect ratio on the results presented in Ref. 1.

III. DESCRIPTION OF EQUIPMENT AND MODELS

The wind tunnel tests of this investigation were carried out in the Cal Tech-Merrill Wind Tunnel at the Pasadena City College. This tunnel is a low speed, closed return type with a rectangular test section two feet by four feet. Maximum dynamic pressure obtainable was about 13.5 lbs. per square foot, which corresponds to a speed of about 72.6 mph. The model was mounted in the normal attitude on a three-strut support with the wing struts attached to trunnions located on the M.A.C. at the maximum thickness point. The rear strut was attached to a tail boom leading back from the wing. The same three points of support were used with or without the fuselage. Force measurements were made on a three-component balance system, measuring lift, drag, and pitching moment simultaneously.

Model Wing.

Dimensional details of the wing may be obtained from Fig. 1. The wing was a double-wedge airfoil section and was milled from a piece of solid annealed brass stock. Leading back from the wing on the axis of symmetry was a solid brass rod to furnish the tail support. For ease of manufacture, the forward and aft surfaces were held as plane surfaces, with equal included angles at the leading and trailing edges when seen in a plane perpendicular to the plane of maximum thickness. This resulted in the plane of maximum thickness occurring at 54% of the chord. No twist or dihedral was incorporated.

The wing configuration was as follows:

Area: 98.3 sq. in.

Aspect Ratio: 3.44

Span: 18.4 in.

Root Thickness: 4.28%

Tip Thickness: 4.55%

Mean Aerodynamic Chord (M.A.C.): 5.54 in.

Sweepback of L. E.: 65°

Sweepback of Quarter Chord Line: 64°

Taper Ratio: .5

The tip thickness is slightly thicker than the root thickness as a result of the ease-of-milling considerations noted above.

Fuselage.

The fuselage was designed by F. Dore and was used in his research work (Cf. Ref. 3), and subsequently used in the experimental work of Ref. 1. Dimensional details may be obtained from Fig. 2. It was made out of mahogany in built-up sections so that the wing could be inserted and clamped in place. The same strut attachment points and method of mounting were used when the wing was tested with the fuselage as with the wing alone. Fillets were built up with the use of modeling clay.

Lift Devices.

The wing high lift devices were made of shim stock or brass sheet, and were secured to the wing with scotch tape, making a smooth

and rigid structure. All flaps were attached to the under side of the wing, and in the case of the split flaps, supporting wedges were fashioned from modeling clay and inserted to maintain rigidity and angular deflections. The nose slats were attached using bent strips of aluminum sheet for support.

The horizontal tail surfaces were the same as those used in Ref. 1 and were mountable in the upper and lower positions. They were attached to the vertical surface with small bolts, and were made of .040 dural sheet. They had an area of 18.2 square inches (18.5% of wing area), an aspect ratio of 1.50, and a leading edge sweepback angle of 65° (Cf. Fig. 9 for dimensional data).

IV. DISCUSSION OF TEST PROGRAM

The maximum dynamic pressure available in the tunnel was about 13.5 lbs. per sq. ft. However, it was found that running at this speed caused considerable vibration in the model and produced a tendency toward coarse readings. As a consequence, all the tests were run using about 8 lbs. per sq. ft. This was further reduced by as much as ten percent as the angle of attack of the model increased to the maximum of 40°. This corresponded to a Reynolds Number of about 244,000, based on the M.A.C.

Force tests were run through a range of angle of attack of -4° through 40° in 4° increments, except where it was deemed advisable to reduce the spacing for more reliable fairing of curves.

Split flaps of 25% chord and of 40, 70, and 100% span were tested at deflections of 20, 40, and 60° throughout the angle of attack range. For the purpose of drawing curves of $C_{L_{max.}}$ versus flap deflection angle, additional runs were made near the stall for deflection angles of 10° and 30°. In all cases, the deflection angles were measured as the angle between the plane of the flap surface and the chord plane of the wing.

Tests similar to the above were run on the extended split flaps except that additional runs for 0° deflection were made in order to measure the effect of the increased area.

Nose flaps of 10 and 20% chord were tested on the wing alone at 20 and 40° deflections. These nose flaps were of 50% span and were

tested in both inboard and outboard positions. Further tests were run on a 100% span nose flap of 10% chord at deflection angles of 20 and 40°.

Two additional nose configurations were tested on the wing alone. These were 50% span nose slats whose chord lengths were constant, one chord measuring 15% of the M.A.C. and the other measuring 23% of the M.A.C. The dimensional data for the nose slats is presented in Fig. 8.

The fuselage was then mounted with the wing, and the testing procedure was repeated. Tests similar to those on the wing without the fuselage were run on the split flaps and extended split flaps, except that only two spans, 40% and 82%, were used. The 82% span was used instead of the 70%, because this carried the flap from the fuselage out to the wing tip.

The horizontal tail surface was tested in the upper position for its effect by itself, and then was tested in both upper and lower positions for its effect in combination with the 40% span extended split flap at a deflection angle of 20°. A 50% span round-nosed nose flap, whose chord length was a constant 15% of the M.A.C., was added to the last combination and its effect noted. Here too, the tail was used in both upper and lower positions.

The round-nosed nose flap was also tested by itself and in combination with the 40% span extended split flap deflected at 20°.

Photographic tuft studies were made of the wing by itself and in combination with the 100% span extended split flap, 70% split flap, 70% extended flap, and the 50% nose flap of 10% chord, all at a flap

deflection angle of 20°. Further photographic studies were made of the wing and fuselage alone and in combination with the 40% span extended split flap, with the round-nosed nose flap, and with the two together. A representative number of these photographs are included in this report. The flow of air at a distance away from the surface of the model was also studied by means of a probe, with a long tuft attached to its end, which was inserted through the tunnel wall into the airstream and held in various positions relative to the model.

V. DISCUSSION OF CORRECTIONS

Since the primary purpose of this investigation was to find the relative effects of various high-lift devices and the general characteristics of the model configurations, rather than the absolute force measurements; and since suitable apparatus such as dummy struts for model inversion was not available, many refinements in the way of corrections were not made. Thus, no zero lift, strut interference, or wall corrections were made. Air density was assumed a constant .00238 slugs per cu. ft. in computing dynamic pressure. However, previous experience in this particular tunnel had indicated that a constant .010 should be subtracted from the drag coefficient. This correction was applied. Previous experience had indicated that the tunnel flow was inclined at about -20 minutes at the struts. This was borne out approximately in this investigation in that a flow inclination of -30 minutes was indicated.

Pitching moments were transferred to an aerodynamic center located at 5.7% of M.A.C. This was determined from the slope of the $C_{m_{tr}}$ versus C_L curve for the wing alone, and was determined in such a way that the moment was relatively constant from an angle of attack of 5° to 20°, rather than using the slope at zero lift, which would have given an aerodynamic center at about 36% M.A.C. The exact slope was hard to determine at the latter point. All force and moment coefficients were based on the area and M.A.C. of the wing alone.

VI. RESULTS AND DISCUSSION

The results of the force measurements are shown in Figs. 12 to 31. Representative photographs of the tuft studies, chosen from the much larger number made, are in Figs. 32 to 48.

Plain Wing and Wing with Fuselage.

The wing alone curves are shown in Fig. 12. The wing by itself gave a $C_{L_{max.}}$ of 1.18. This compares with two-dimensional results, given in Ref. 4 and 5, of from .7 to .8, or somewhat less than twice that for a two-dimensional wing. However, as might be expected from the high sweep-back, the angle of attack for maximum lift was quite high and was generally at 38°. This was about three times as great as the angle of attack for maximum lift coefficient for the two-dimensional results.

The pitching moment characteristics of the wing alone were generally satisfactory and were fairly constant in an angle of attack range of 5 to 20°. As noted before, the aerodynamic center was chosen at 5.7% of the M.A.C. because of this constancy in what might be considered the working range. If the slope of the $C_{M_{tr}}$ versus C_L curve at zero lift had been taken to determine the aerodynamic center, a wide variation in the moment curve would have resulted, for that center would have been at about 36% of the M.A.C. It was felt that moments calculated at the aft point would lead to misleading conclusions as to the stability of the wing. Slopes of the moment curve

calculated about the 5.7% point are in the stable direction except at the stall. Pitching moment coefficients for all other configurations in this report are given about this 5.7% point.

An analysis of the moment curve and the tuft studies shows that the wing stalls progressively in from the tips, but shows no inclination toward abrupt stall at 38 to 40° which was the maximum angle of attack tested.

The addition of the fuselage to the wing produced an increase in the slope of the lift curve and an increase in $C_{L_{max.}}$ of from 1.18 to 1.3 (Cf. Fig. 13). The presence of the fuselage did not produce any general change in the moment characteristics, but did seem to remove the unstable tendency at the stall.

Split Flaps.

The results of the split flaps without the fuselage are presented in Figs. 14 to 16. It may be seen from these figures that the split flaps gave increases in lift over the lower range of attack angle, but only in the case of the 100% span flap was the $C_{L_{max.}}$ increased, and there only by .02. The 40 and 70% spans actually lowered the maximum lift coefficient. The increments of lift in the lower range due to the flap deflection were not proportional to deflection angle, by far the largest increment, in proportion, being furnished by 20° deflection. The transition region, in the middle range, indicated a decided change in flow conditions which produced marked effects on the moment and lift curves.

The moments were, of course, of greater magnitude but showed

stable tendencies, except in the transition range where decided reversals occurred. This conforms with the results presented in Refs. 1 and 6.

The results produced by the addition of the fuselage are shown in Figs. 17 and 18. The same general effects of the split flaps were noted here, but with a more favorable effect on the lift in the lower ranges. The 82% span flap produced the only increase in $C_{L_{max.}}$. Apparently the flow conditions were not radically changed by the presence of the fuselage, and increases in lift generally corresponded with those resulting from the addition of the fuselage to the wing, previously noted. The moment curves were of the same general form, but the fuselage had the effect of smoothing out the curves.

Extended Split Flaps.

The results of adding the extended split flaps to the wing are shown in Figs. 19 to 21. These flaps, of course, increased the area of the wing and this effect may be noted from the curve of 0° deflection, where it may be seen that the slope of the lift curve is considerably greater. The lift was increased throughout the range, with 20° flap deflection having the largest effect on $C_{L_{max.}}$. Here again the lift increments were not proportional to the deflection angle, the greatest increment, in proportion, being produced by 20° deflection. The same transition region occurred as in the case of the split flaps but at a higher angle of attack. In general, the extended split flaps were much more effective in increasing the lift than were the split flaps, and were decidedly effective in increasing

$C_{L_{max.}}$. For instance, $C_{L_{max.}}$ for the 100% span extended split flap was 1.64 as compared to 1.18 for the wing alone. The moment curves were of the same general form as the split flaps, but the magnitude of the moments was considerably greater, as could be expected. For instance, the 100% span flap gave a moment coefficient of -.55 at 40° flap deflection and 40° angle of attack. The slopes were stable in tendency at the stall.

The effect of adding the fuselage may be seen in Figs. 22 and 23. The extended split flaps had the same general effect in the presence of the fuselage as with the wing alone. The maximum lift coefficient was increased slightly to 1.68 in the case of the 82% span flap at a deflection of 20°. The presence of the fuselage produced no particular change in the moment characteristics in this case.

Nose Flaps and Slats.

The results obtained by adding these devices to the wing may be seen in Figs. 24 to 27. The nose flaps increased the lift in the upper range of angle of attack, and, without exception, increased $C_{L_{max.}}$ over that of the wing alone. In the case of the 50% span nose flap, in the inboard position, at a deflection of 40°, the maximum lift was increased to 1.4. This points out the advisability of improving the flow over the sharp leading edge. It should be further noted that the nose flaps were much more effective in the inboard position in improving maximum lift. The nose slats tested had very little effect except to improve maximum lift slightly. However, more extensive experimentation in this line would probably produce more

desirable results.

When mounted in the outboard position the nose flaps and slats produced stable tendencies in the moment characteristics at the stall. The 50% span nose flaps produced more positive moments when mounted in the inboard position, and more negative moments when mounted outboard. These devices seem to be a possible source of improvement in the stability characteristics of an airplane of this type.

The round-nosed nose flap will be discussed under Miscellaneous Configurations.

Miscellaneous Configurations.

The results of tests on these miscellaneous configurations may be seen in Figs. 28 to 31. The addition of the horizontal tail to the fuselage increased $C_{L_{max.}}$ from 1.3 to 1.43 at 40° angle of attack. The magnitude of the moment was increased from -.2 to -.55 at 40° with stabilizing tendencies throughout.

The fuselage, horizontal tail, and 40% span extended split flap produced a general increase in lift over the whole range, as compared to the wing and fuselage only. The presence of the tail increased $C_{L_{max.}}$ from 1.52 to 1.68. The effect of the extended split flap was to increase $C_{L_{max.}}$ from 1.43 to 1.60 when the tail was in the upper position. The moment was large but stabilizing at high lift.

The round-nosed nose flap tested with the wing and fuselage, decreased the lift except at angles of attack above 33°, above which a very slight increase was experienced, and it had little effect on the moment (Cf. Fig. 30). Adding the 40% span extended split flap to

this combination produced an increment in maximum lift coefficient of .3, which was .06 more than could be expected from adding the separate increments. The most noteworthy feature of this configuration was the almost complete elimination of the irregularity in the transition region of the moment curve.

The combination of the fuselage, horizontal tail surface, 40% span extended split flap, and round-nosed nose flap (Cf. Fig. 31) produced a $C_{L_{max.}}$ of 1.78 which was the highest lift coefficient for the configurations tested. This was an increase of .48 over the wing with fuselage only, and an increase of .6 over the wing alone. This combination was tested with the horizontal tail surface in both the upper and lower positions, with the lower position giving a slightly greater lift at high angles of attack. The upper tail position gave a slightly more negative moment from 8 to 26° angle of attack, but the moment curves fall on top of each other above 26°. Although there is a sharp change in slope, in a stable direction, above 26° angle of attack, and although the moment increases to -.71 at $C_{L_{max.}}$, the curve is generally satisfactory, and the dip which occurs when the nose flap is not present was almost eliminated.

General Discussion.

Special attention was given to the problem of determining the flow conditions which produced the transition region, causing dips in the lift and moment curves when the split and extended split flaps were used.

The wing with the 70% span split flap deflected at 20° will be

considered. Photographs of surface tuft studies for this configuration are included in Figs. 32 to 37. At zero angle of attack all the tufts are smooth and are streaming fore and aft. At an angle of attack of 8° one tuft close to the nose has begun to fluctuate violently. Most of the other tufts are deflected in a spanwise direction, especially at midspan. At 12° the effects noted previously are more marked. Several more tufts near the nose are fluctuating. Those at midspan, aft of the leading edge row, are even bent forward of the maximum section line. The lift and moment curves at this stage are beginning to show some uncertainty (Cf. Fig. 15). However, no spanwise section of the wing could be said to be stalled, in that turbulent flow is not present except at the nose. At 16° and 20°, the tufts near the nose are fluctuating with greater violence, and there is a scattering of fluctuating tufts near midspan. At 24° some of the tufts that were previously fluctuating have begun to settle down, except near the nose. It should be noted that the tufts near the tip are still fairly smooth.

The investigation of the flow at a distance away from the surface of the wing, by means of a probe, revealed that a vortex was being shed, starting just aft of the nose and passing over the trailing edge at about the two-thirds span point. This conforms with the surface tuft indications. This vortex was quite violent and the very clear-cut cone formed by the revolving tuft had an included angle of about 40° after it passed over the trailing edge of the wing. The presence of this phenomenon seemed to coincide with the occurrence of irregularities in the lift and moment curves.

VII. CONCLUSIONS

The results of tests at low speed of a 3.44 aspect-ratio, tapered, 65° swept-back, high speed wing indicate that for the configurations tested:

1. The maximum lift coefficient of the swept-back wing was approximately 65% higher than that shown in the two-dimensional airfoil section data. However, it was reached at a very much greater angle of attack which is usual with the highly swept-back wings.

2. The split flaps were effective in increasing lift in the lower ranges of angle of attack. For high $C_{L_{max.}}$ the optimum flap deflection angle was 20° when tested with the wing and 40° when tested with the wing and fuselage.

3. The extended split flaps were much more effective in increasing the lift coefficient than were the split flaps. The optimum flap deflection angle for $C_{L_{max.}}$ was 20°.

4. Nose flaps increased the lift coefficient in the upper ranges of angle of attack and increased $C_{L_{max.}}$. They also improved the flow over the wing as was evident from the smoothing out of the moment curves.

5. The combination of the wing, fuselage, horizontal tail surface, 40% span extended split flap, and round-nosed nose flap produced a maximum lift coefficient of 1.78 which was the highest obtained with the configurations tested.

6. Below the stall, the moments had stable tendencies, except

where irregularities in the lift curve occurred. These irregularities were apparently caused by a vortex shedding from a point just aft of the nose of the wing.

7. The fuselage had the effect of increasing the slope of the lift curves and was a stabilizing influence at the stall.

8. The horizontal tail surface increased $C_{L_{max}}$ and had a marked stabilizing effect on the moment.

VIII. REFERENCES

1. Jensen, A. J., and Koerner, W. G.: Wind Tunnel Investigation of a Supersonic Tailless Airplane at Low Subsonic Speed. Thesis, California Institute of Technology (1948).

2. Blenkush, P. G., and Densmore, J. E.: Wind Tunnel Investigation of the Aerodynamic Characteristics of High-Lift Devices on Supersonic Wings at Low Subsonic Speed. Theses, California Institute of Technology (1949).

3. Dore, F.: The Design of Tailless Airplanes. Thesis, California Institute of Technology (1947).

4. Pollock, A. D., Jr., and Reck, F. F.: A Study of Methods to Increase the Lift of Supersonic Airfoils at Low Speed. Thesis, California Institute of Technology (1947).

5. Hilton, W. F., and Pruden, F. W.: Subsonic and Supersonic High Speed Tunnel Tests of a Faired Double-Wedge Aerofoil. R. & M. #2057 (Dec., 1943).

6. Lowry, J. G., and Schneiter, L. E.: Investigation at Low Speed of the Longitudinal Stability Characteristics of a 60° Swept-Back Tapered Low-drag Wing. N.A.C.A. T.N. #1284 (May, 1947).

FIG. 1

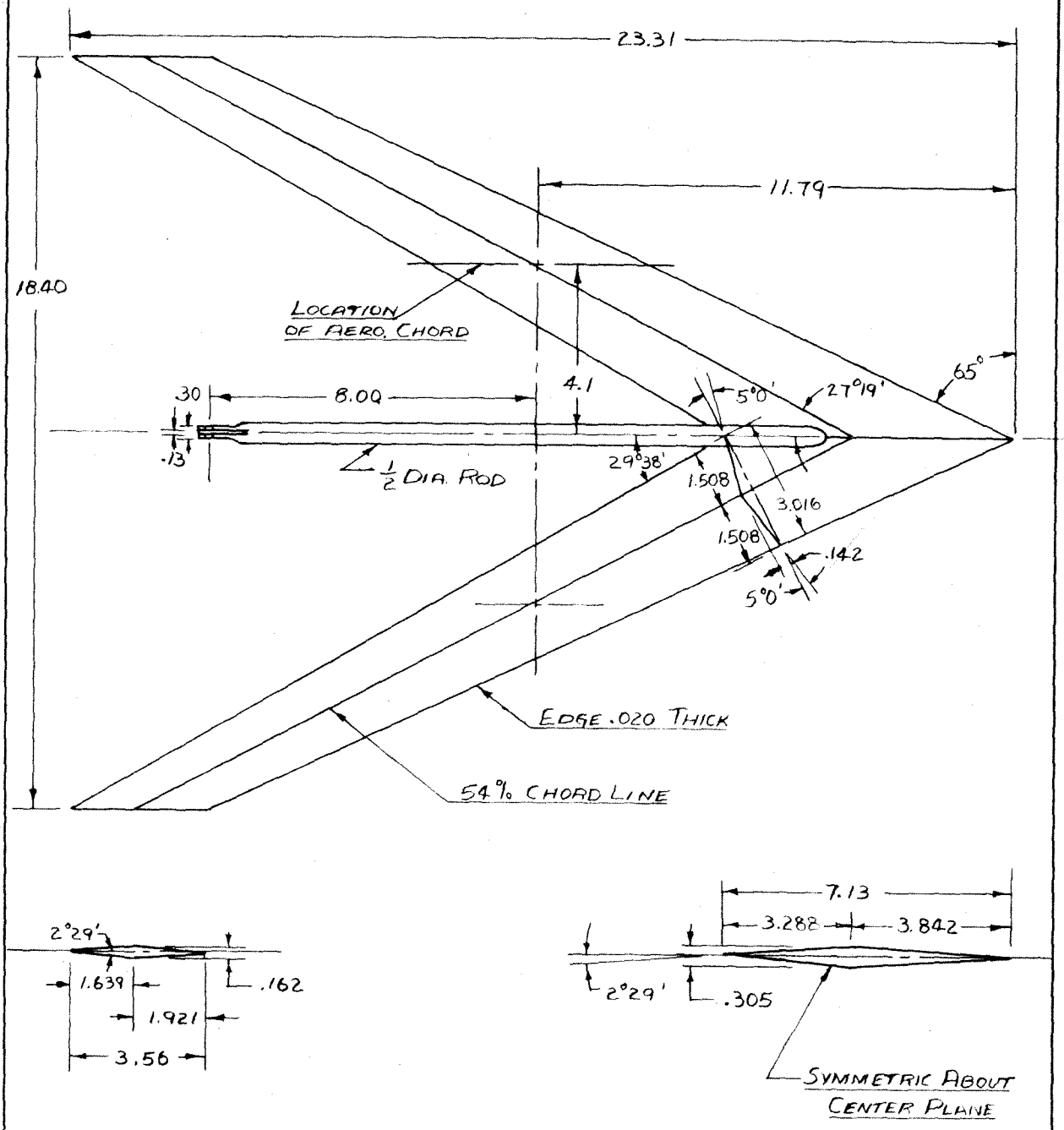

SWEPT BACK WING

AREA: 98.3 SQ. IN.
ASPECT RATIO: 3.44
SPAN: 18.4 IN.
ROOT THK'S: 4.28 %
TIP THK'S: 4.55 %
M.A.C.: 5.54"
SWEEPBACK L.E.: 65°
SWEEPBACK ¼ CHORD LINE: 64°
TAPER RATIO: .5

FIG. 2

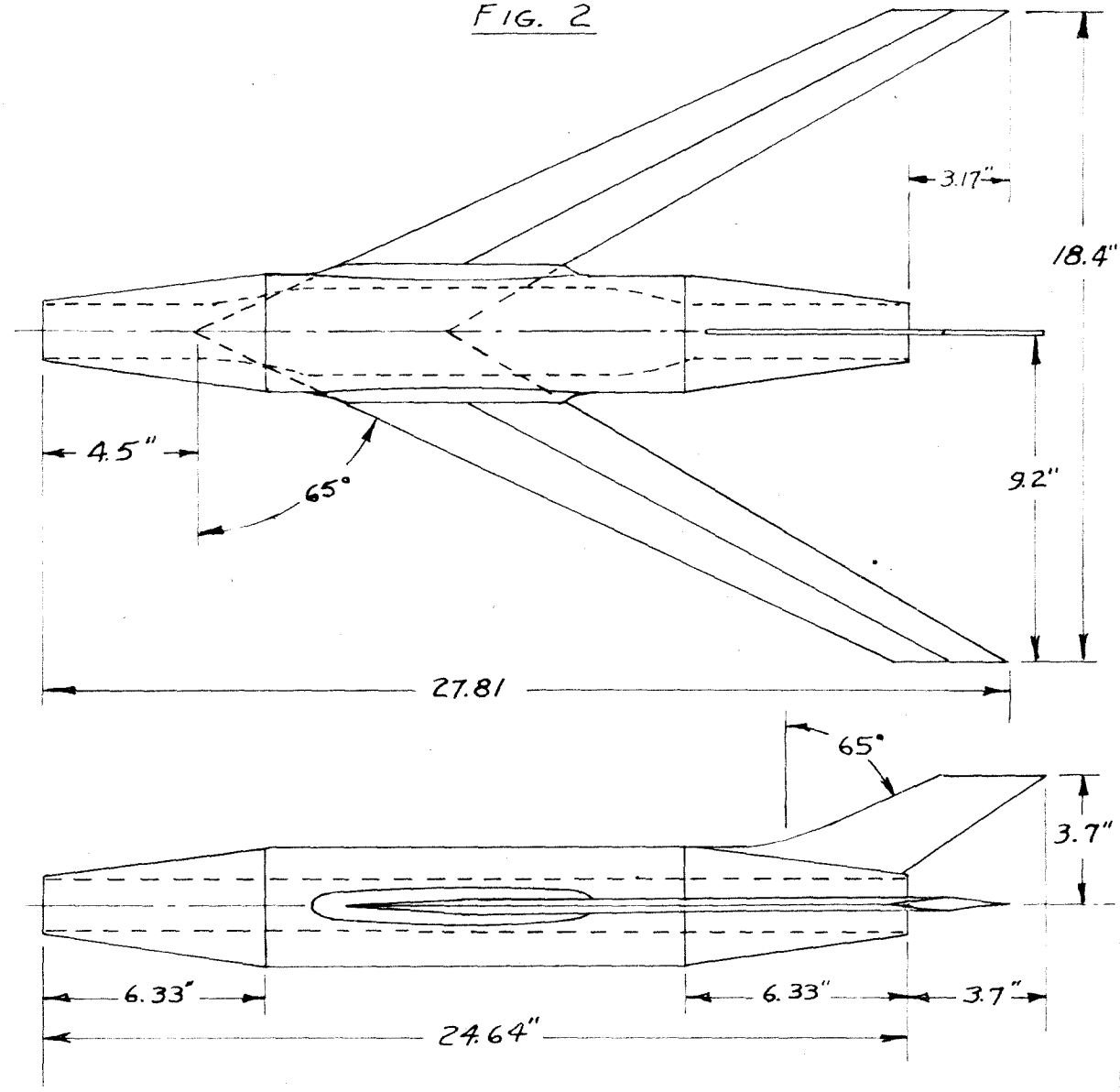

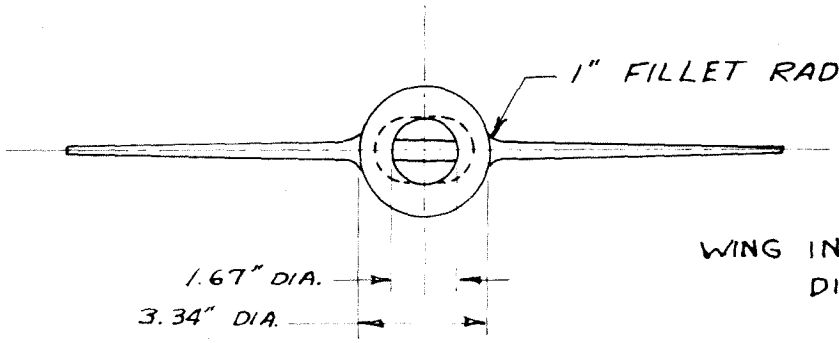

WING INCIDENCE: 0°
DIHEDRAL : 0°

SWEPT-BACK WING WITH FUSELAGE

FIG. 3

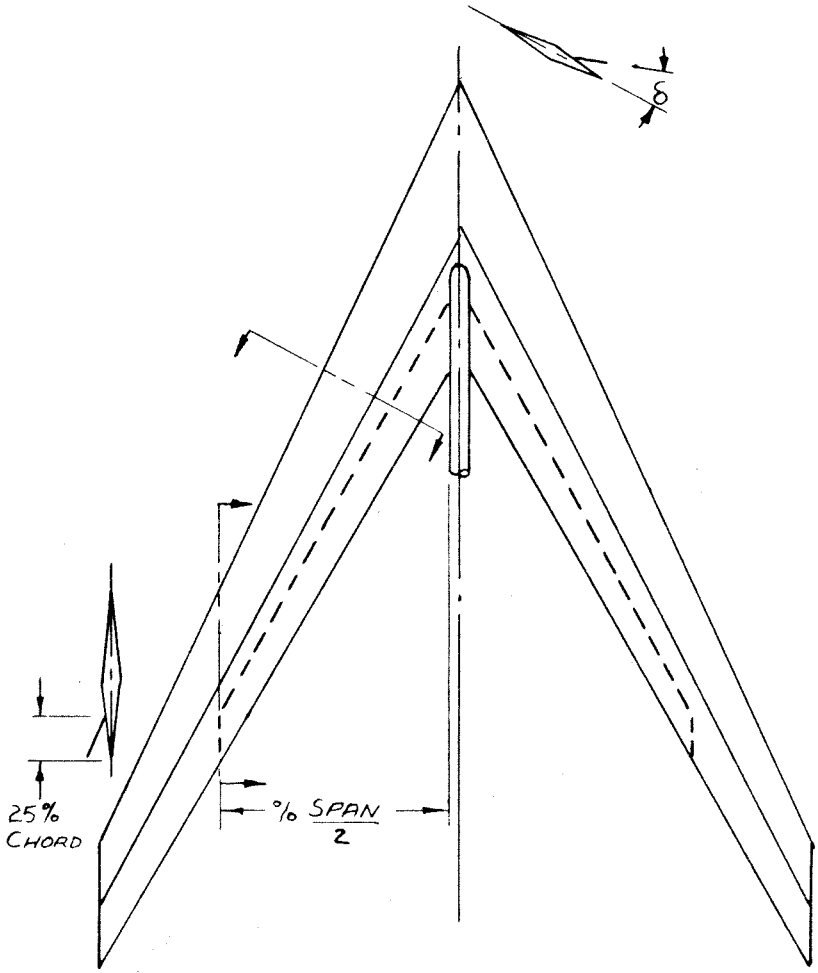

SWEPT BACK WING WITH SPLIT FLAPS

SPAN	% WING AREA
40	10
70	17.5
100	24.3

FIG. 4

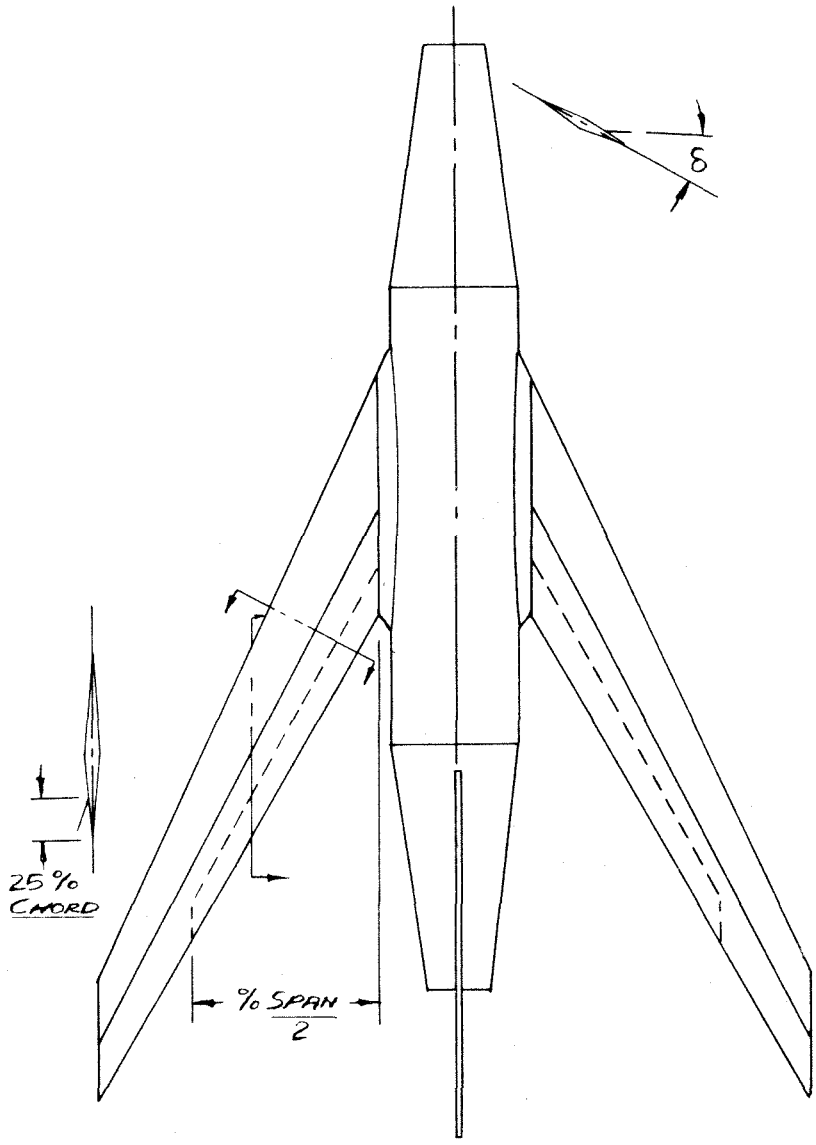

SWEPT BACK WING WITH FUSELAGE AND SPLIT FLAPS

SPAN	% WING AREA
40	10
82	20.5

FIG. 5

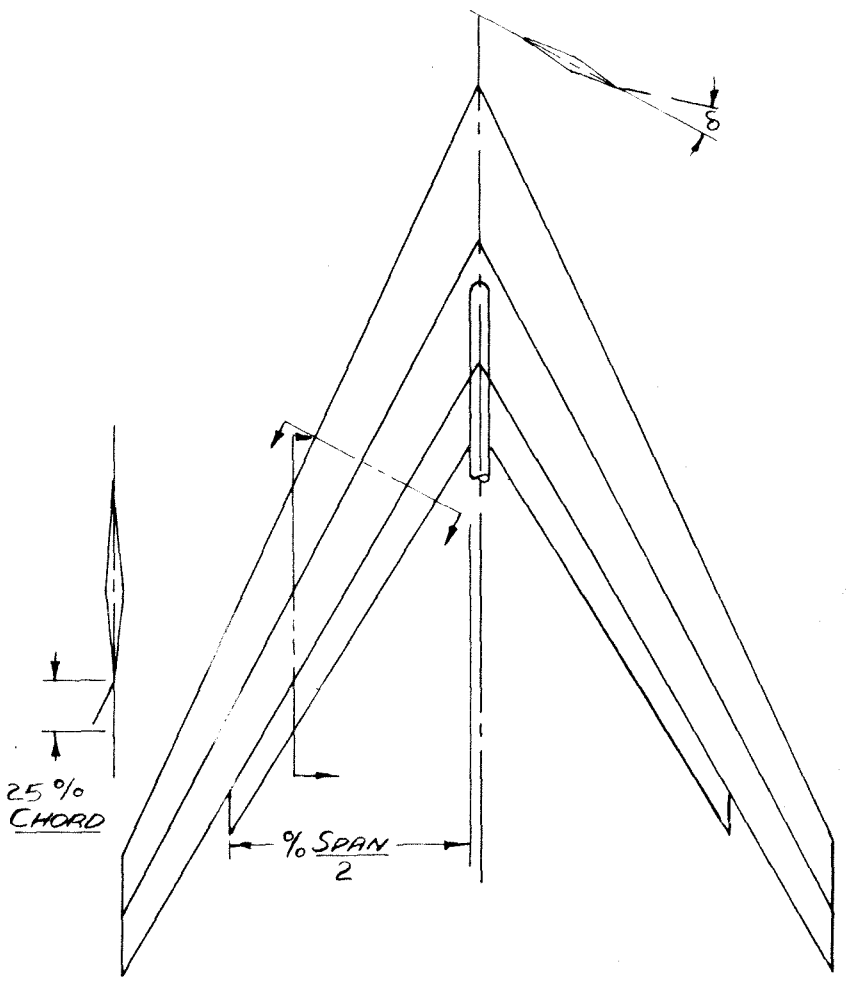

SWEPT BACK - WING WITH EXTENDED SPLIT FLAPS

SPAN	% WING AREA
40	10
70	17.5
100	24.3

FIG. 6

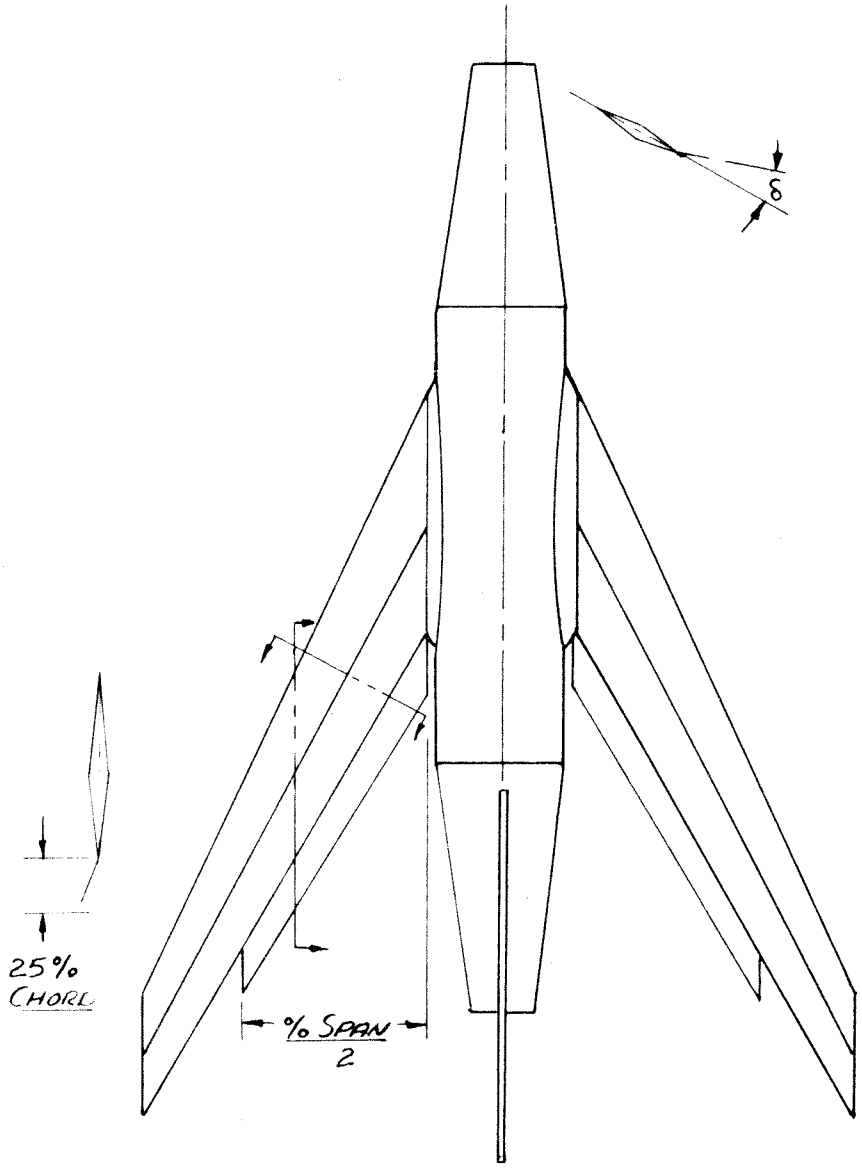

SWEPT BACK WING WITH FUSELAGE
AND EXTENDED SPLIT FLAPS

% SPAN	% WING AREA
40	10
82	20.5

FIG. 7

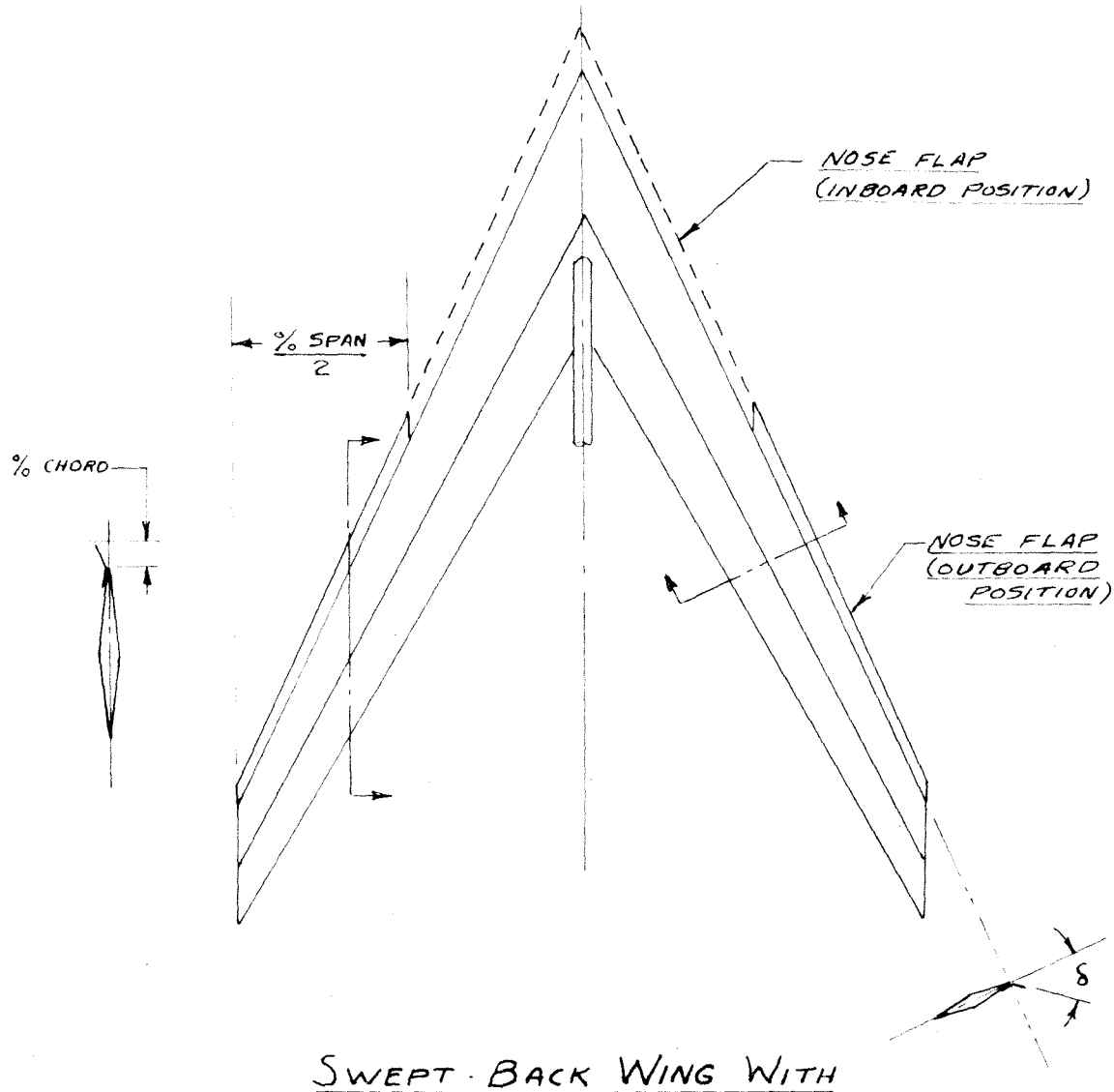

SWEPT-BACK WING WITH NOSE FLAPS

% SPAN	% CHORD	% WING AREA
50	10	5
50	20	10
100	10	10

FIG. 8

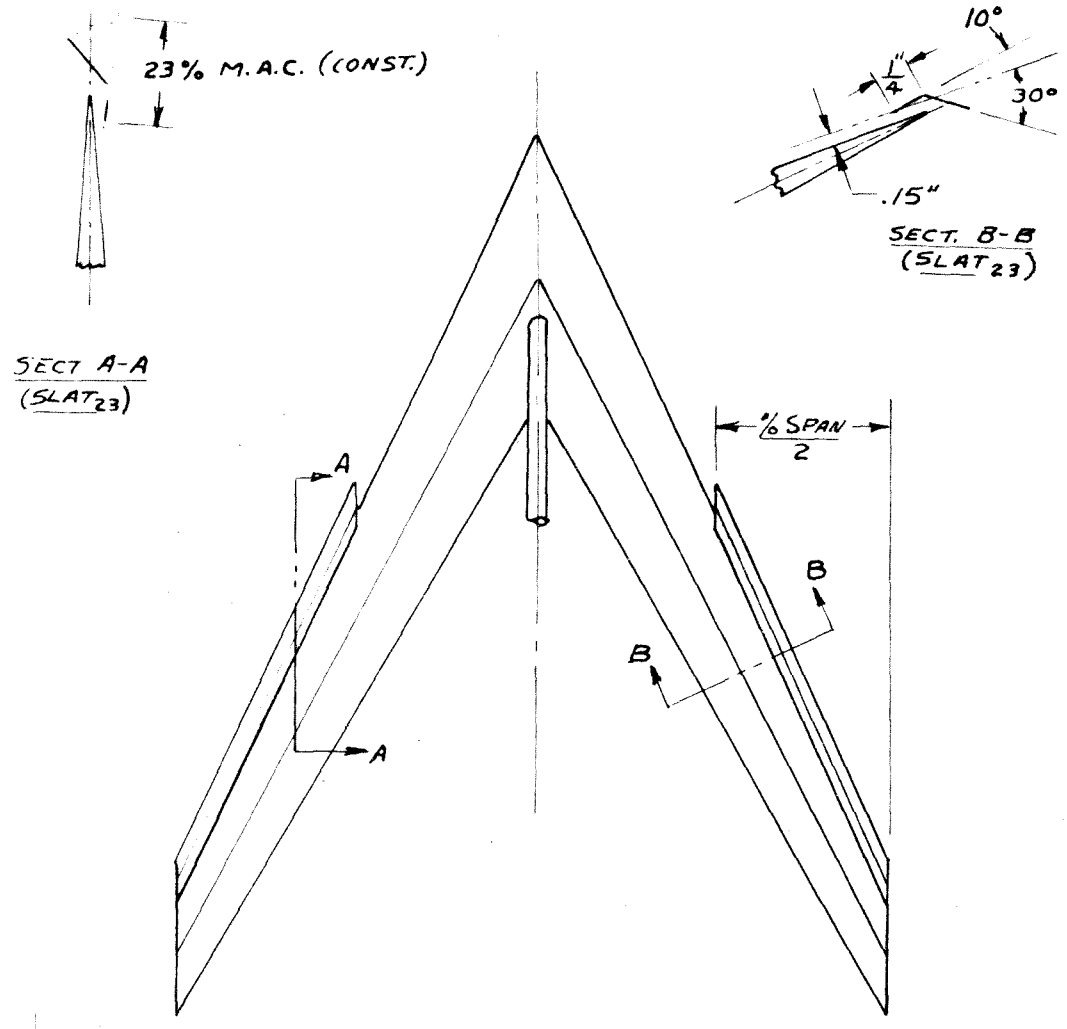

SWEPT-BACK WING WITH NOSE SLATS

% SPAN	% M.A.C.	% WING AREA
50	15	7.8
50	23	11.9

FIG. 9

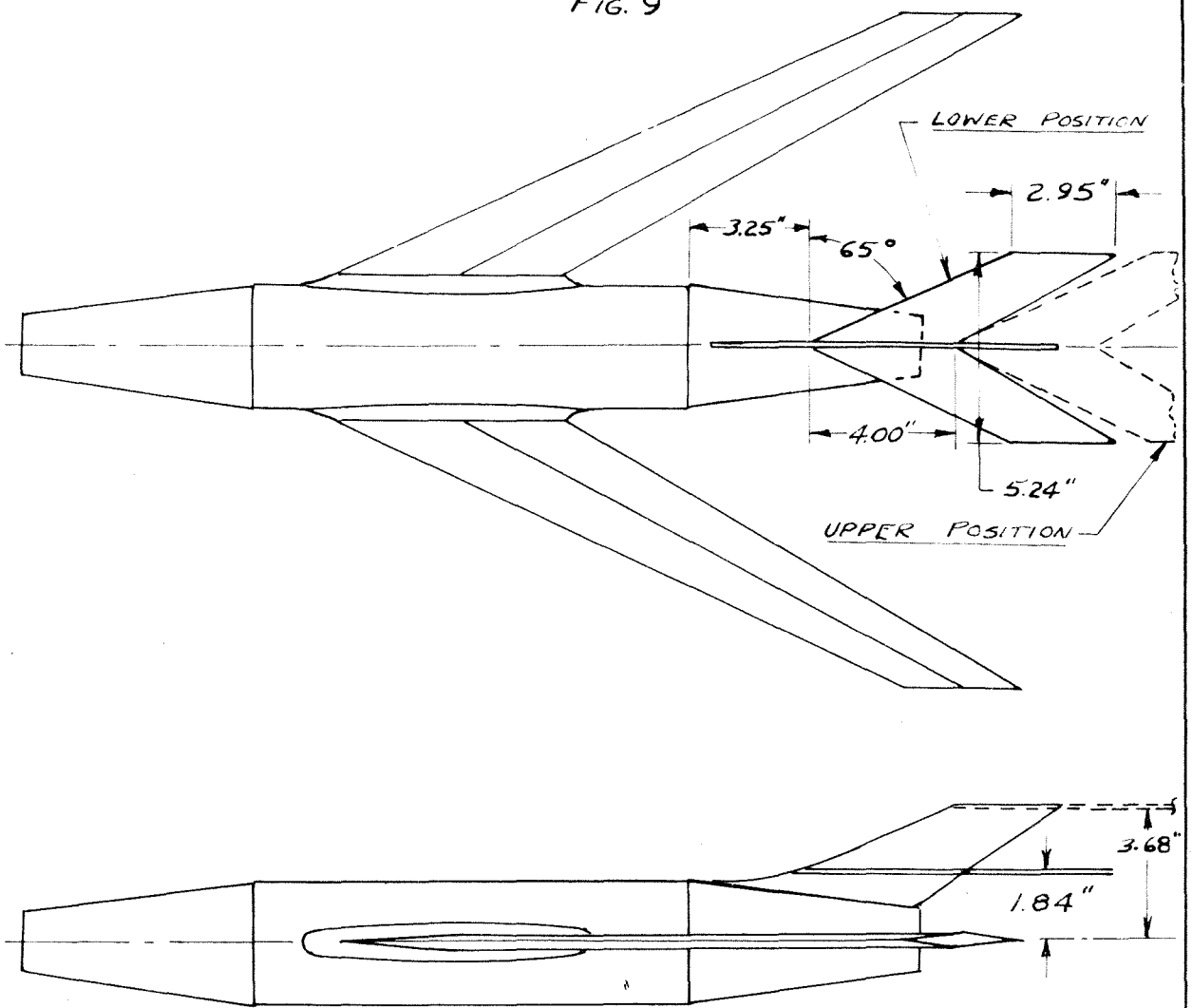

SWEPT-BACK WING WITH FUSELAGE
AND HORIZONTAL TAIL SURFACE

HORIZONTAL TAIL SURFACE:
AREA: 18.5% OF WING AREA
ASPECT RATIO: 1.5

FIG. 10

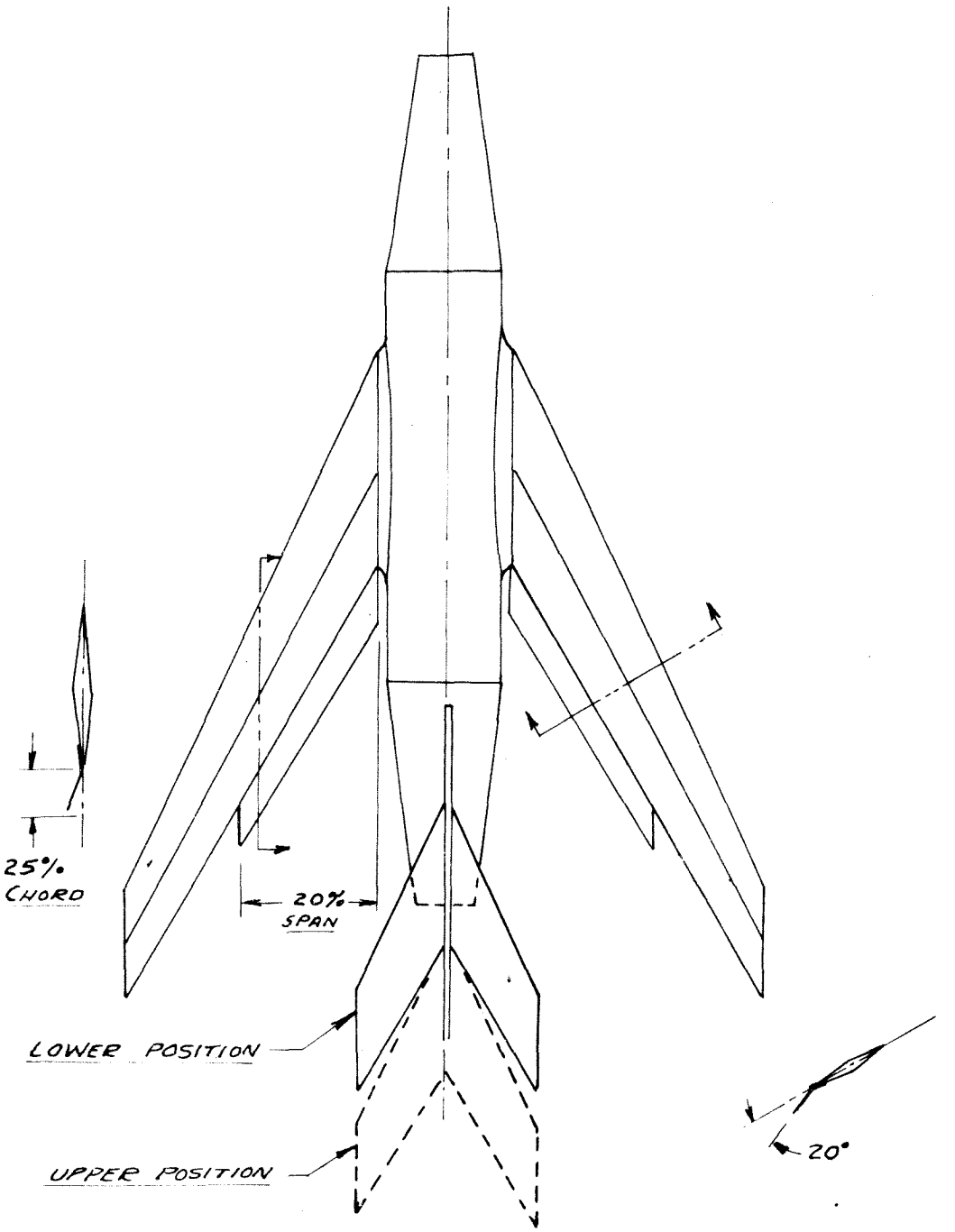

SWEPT-BACK WING WITH FUSELAGE, HORIZONTAL TAIL SURFACE, AND 40% SPAN EXTENDED SPLIT FLAP

	% OF WING AREA
HORIZONTAL TAIL SURFACE:	10
40% SPAN FLAP	18.5

FIG. 11

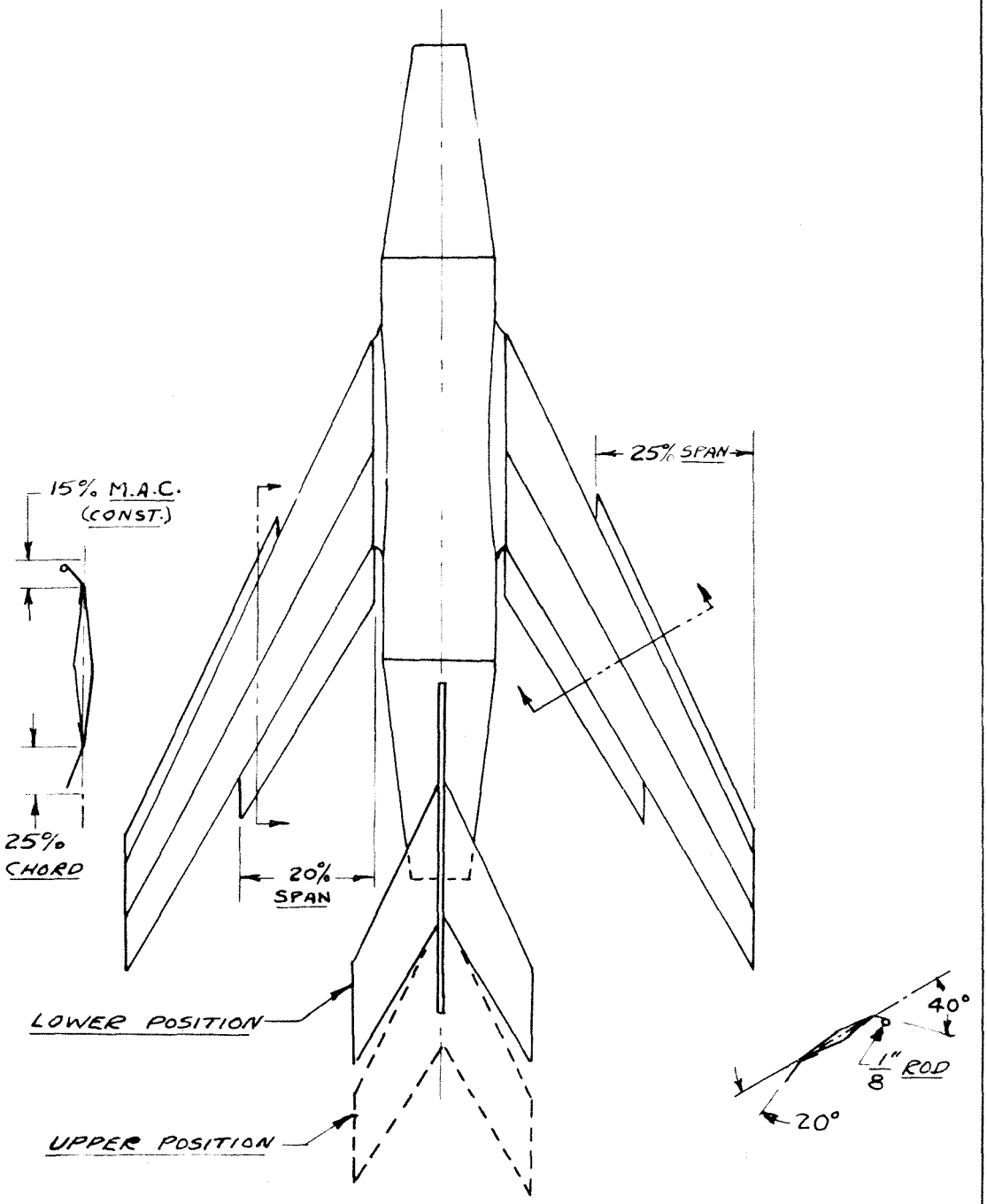

SWEPT-BACK WING WITH FUSELAGE, HORIZONTAL TAIL SURFACE, 40% SPAN EXTENDED SPLIT FLAP, AND 50% SPAN ROUND-NOSED NOSE FLAP

	% OF WING AREA
HORIZONTAL TAIL SURFACE:	18.5
40% SPAN EXTENDED SPLIT FLAP:	10
50% SPAN ROUND-NOSED NOSE FLAP:	7.8

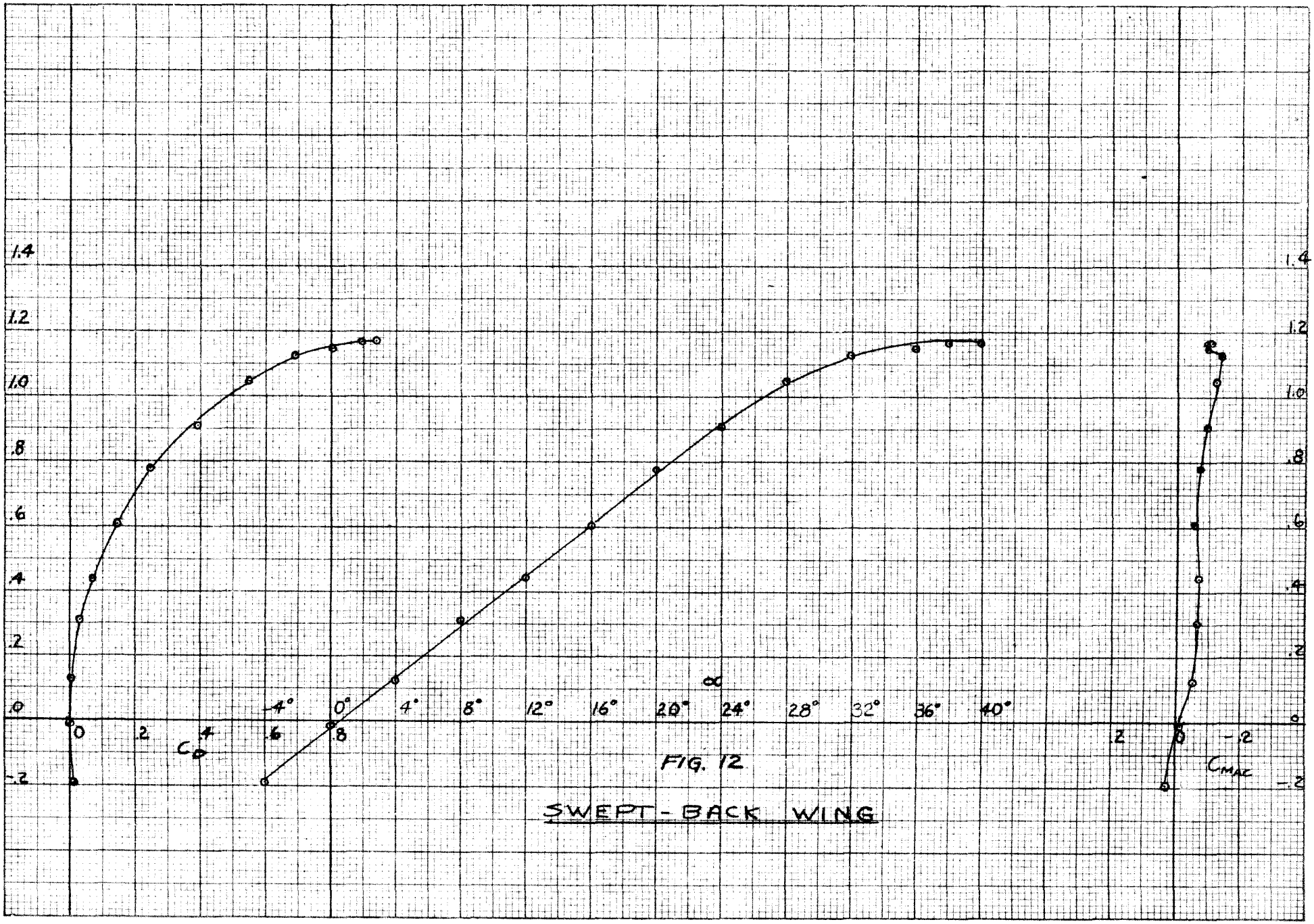

FIG. 12

SWEPT-BACK WING

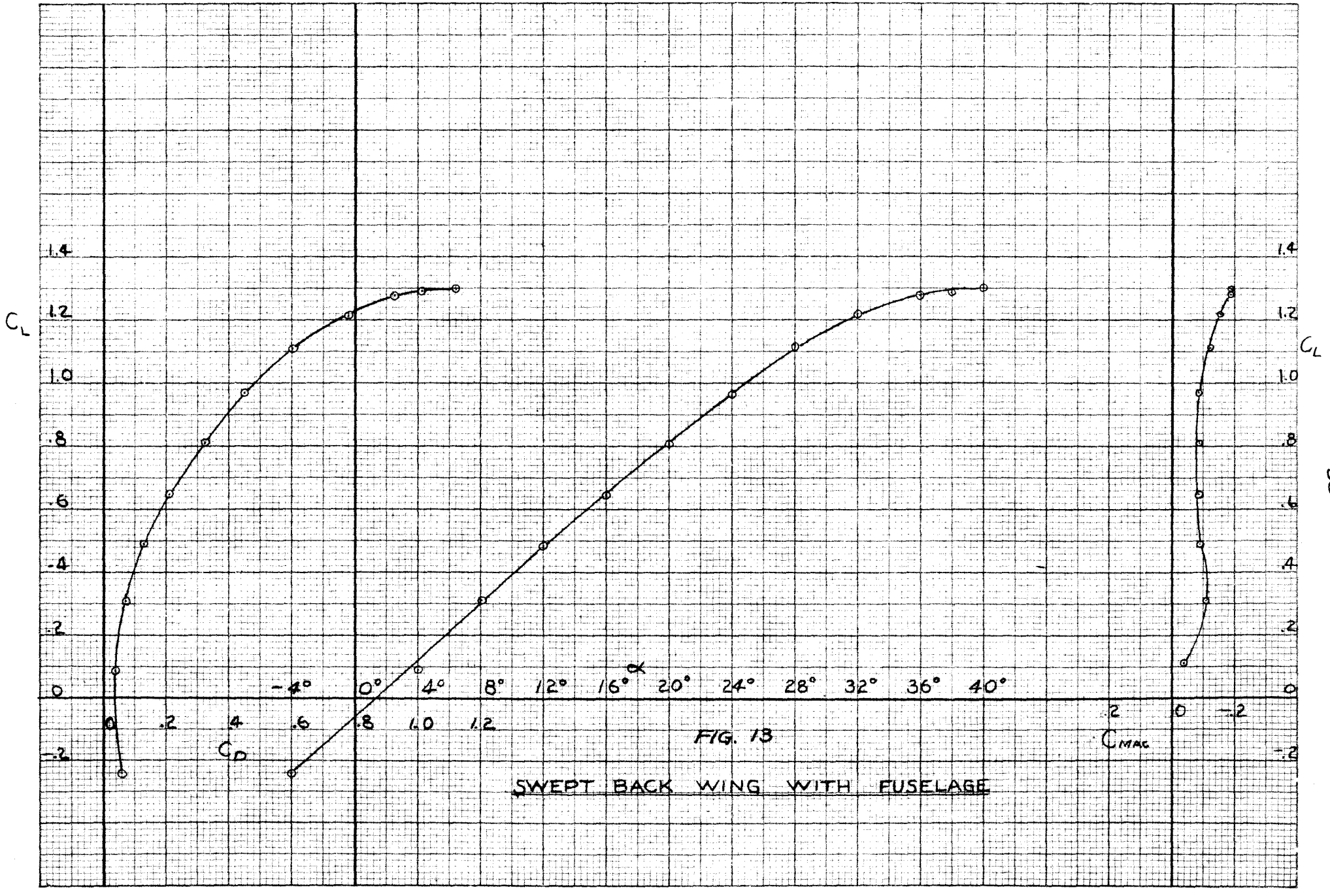

FIG. 13

SWEPT BACK WING WITH FUSELAGE

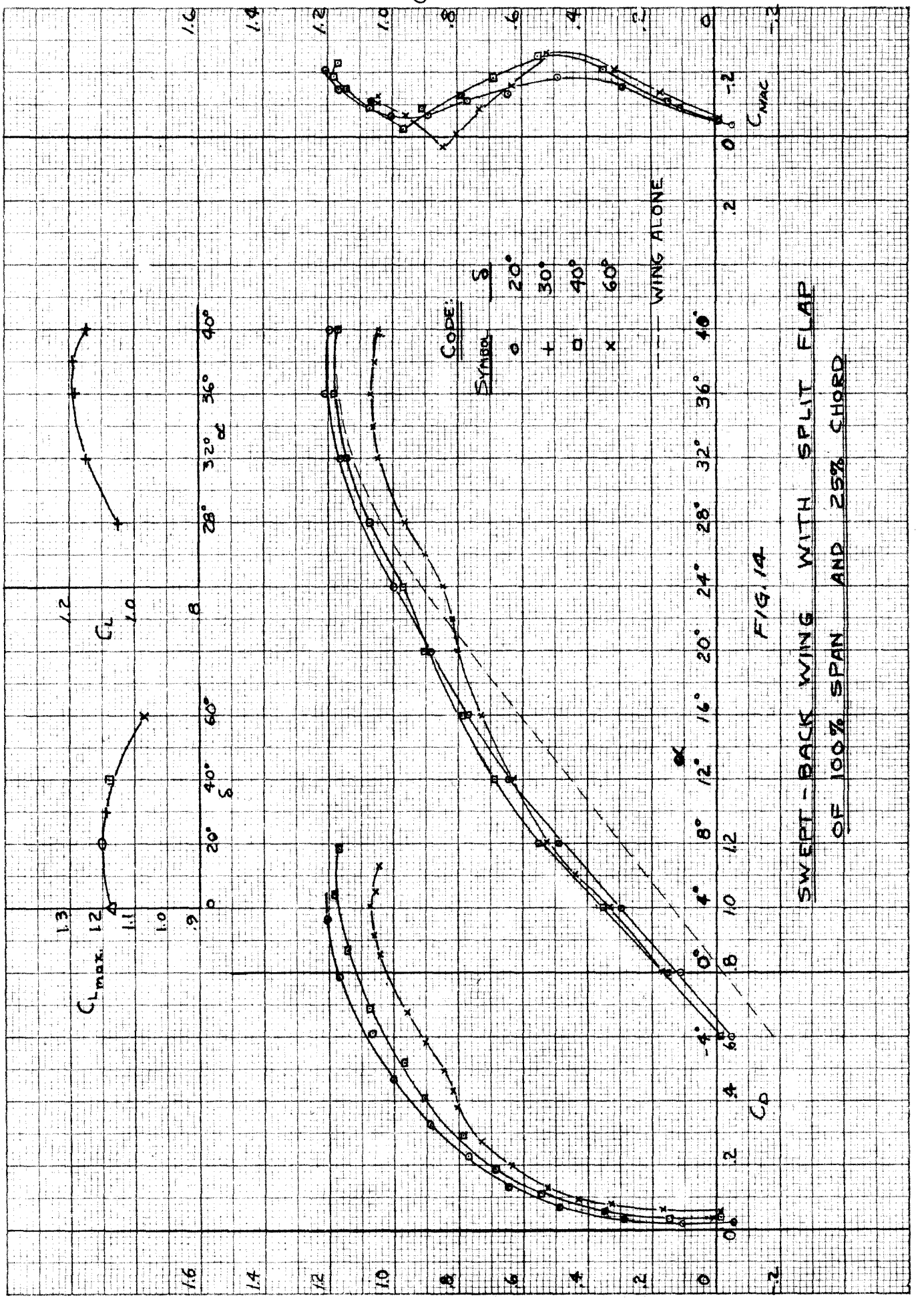

FIG. 14

SWEPT-BACK WING WITH SPLIT FLAP
OF 100% SPAN AND 25% CHORD

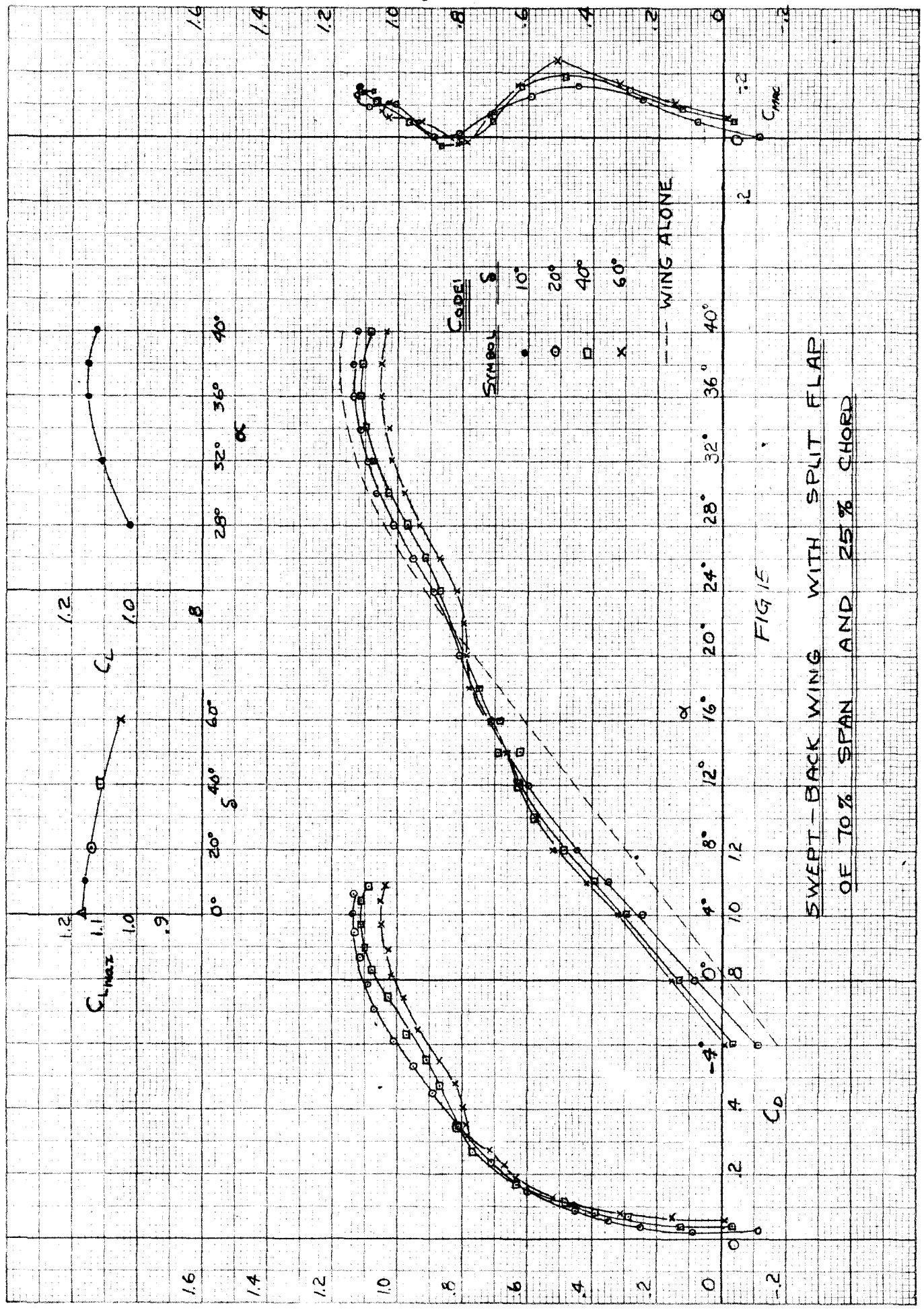

FIG 15

SWEPT-BACK WING WITH SPLIT FLAP OF 70% SPAN AND 25% CHORD

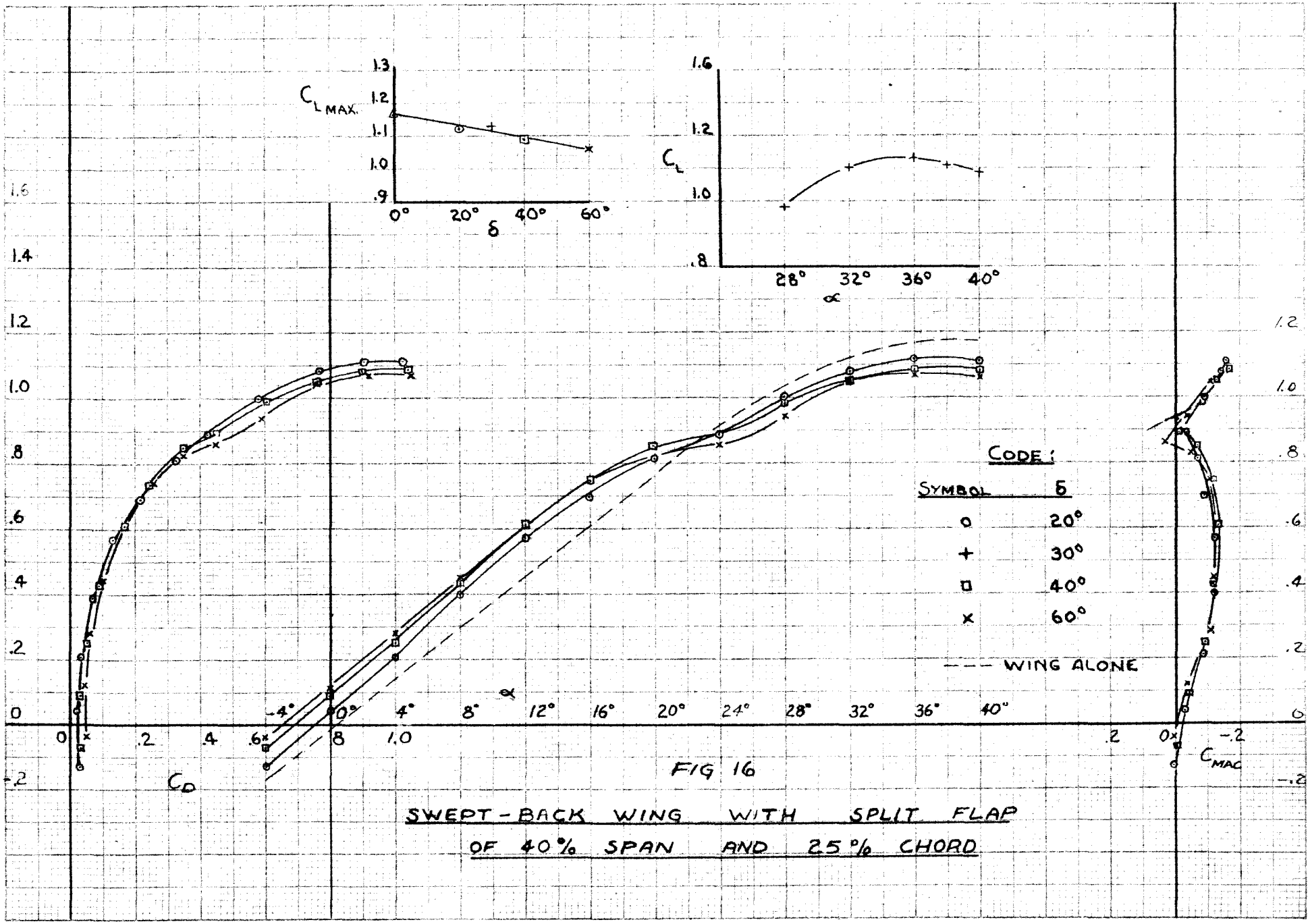

FIG 16

SWEPT-BACK WING WITH SPLIT FLAP
OF 40% SPAN AND 25% CHORD

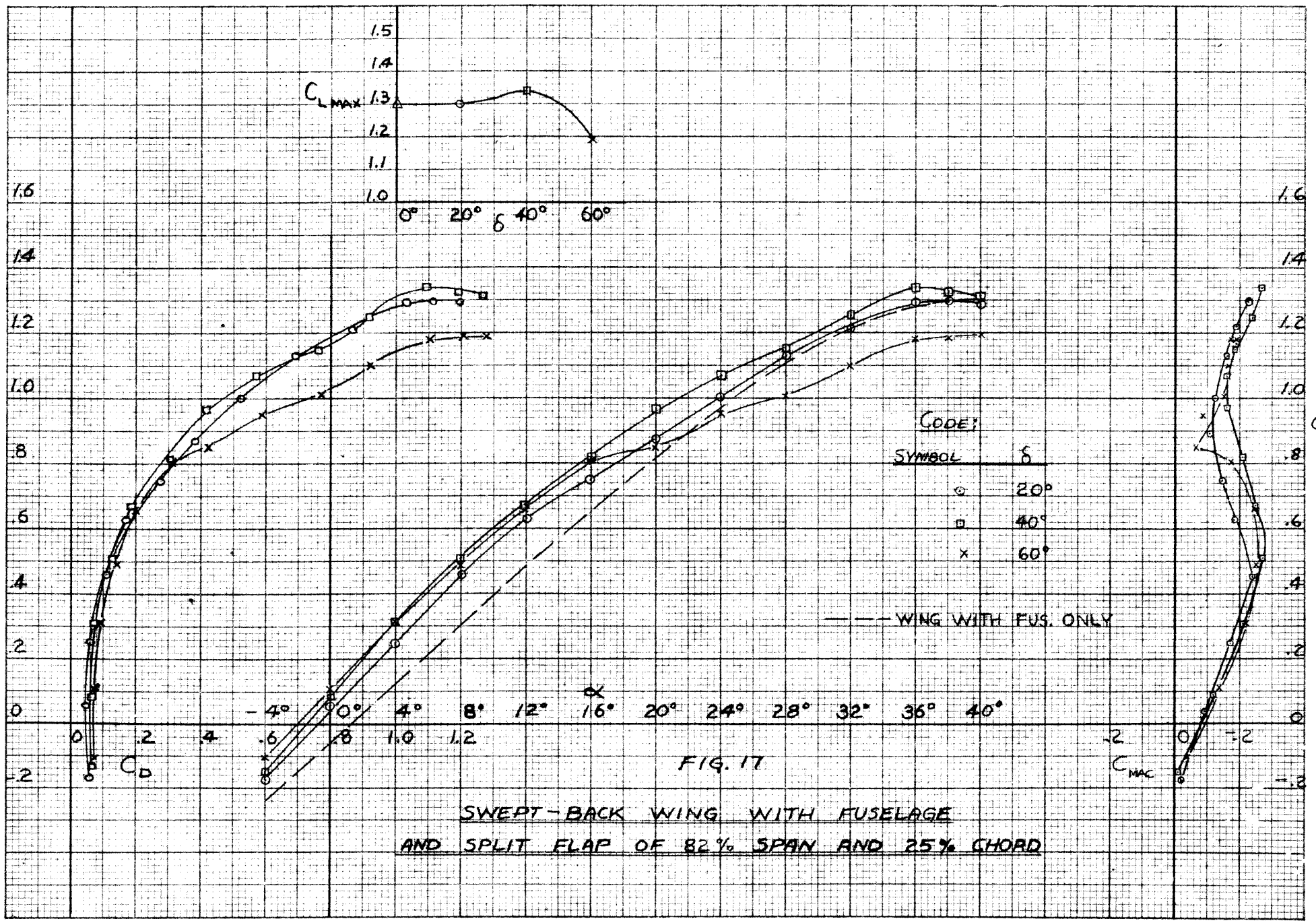

FIG. 17

SWEPT-BACK WING WITH FUSELAGE AND SPLIT FLAP OF 82% SPAN AND 25% CHORD

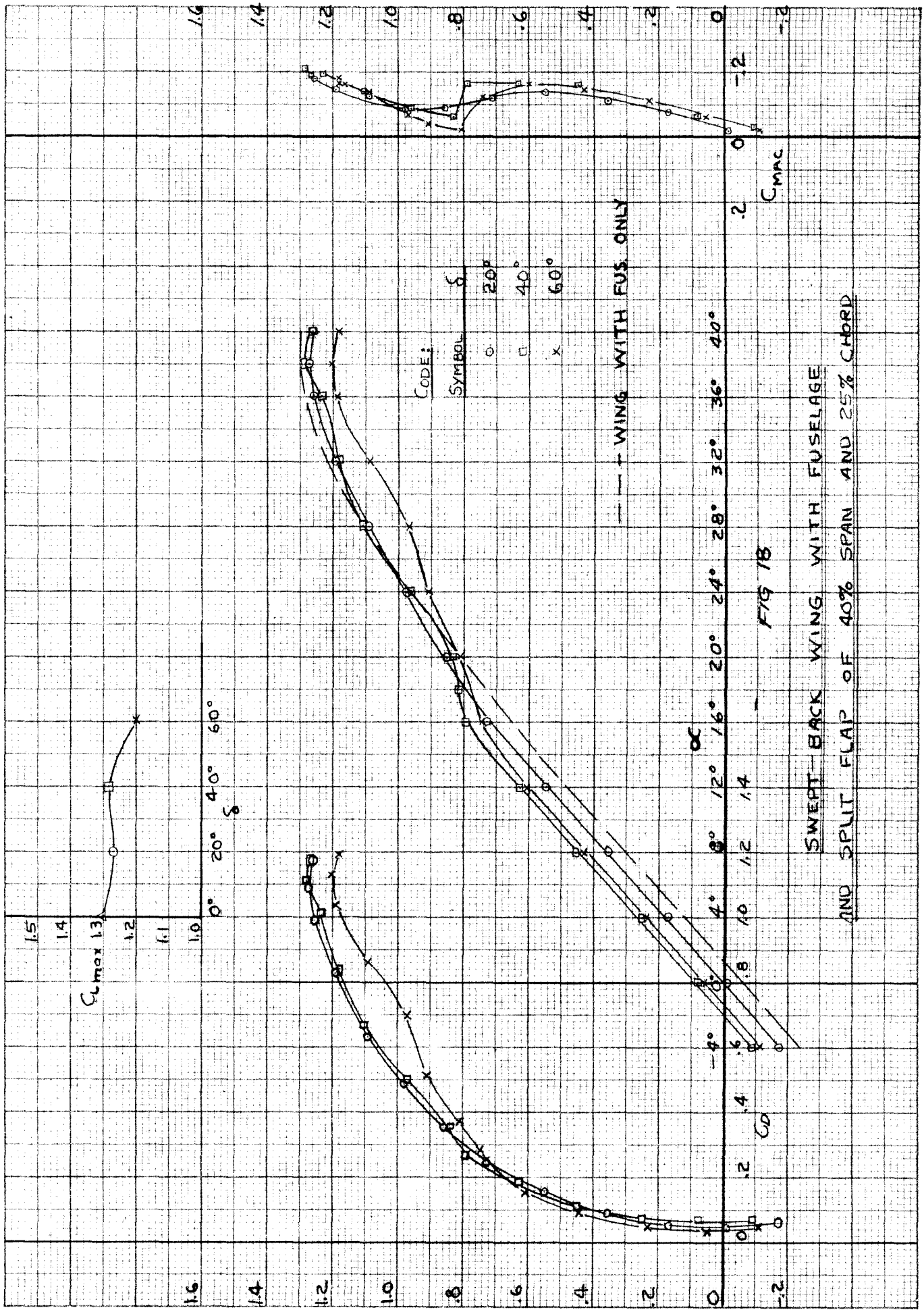
SWEPT-BACK WING WITH FUSELAGE
AND SPLIT FLAP OF 40% SPAN AND 25% CHORD
WING WITH FUS. ONLY
CODE:
SYMBOL δ
20°
40°
60°
FIG 18
α
CL
CD
Cmac
CLmax
δ

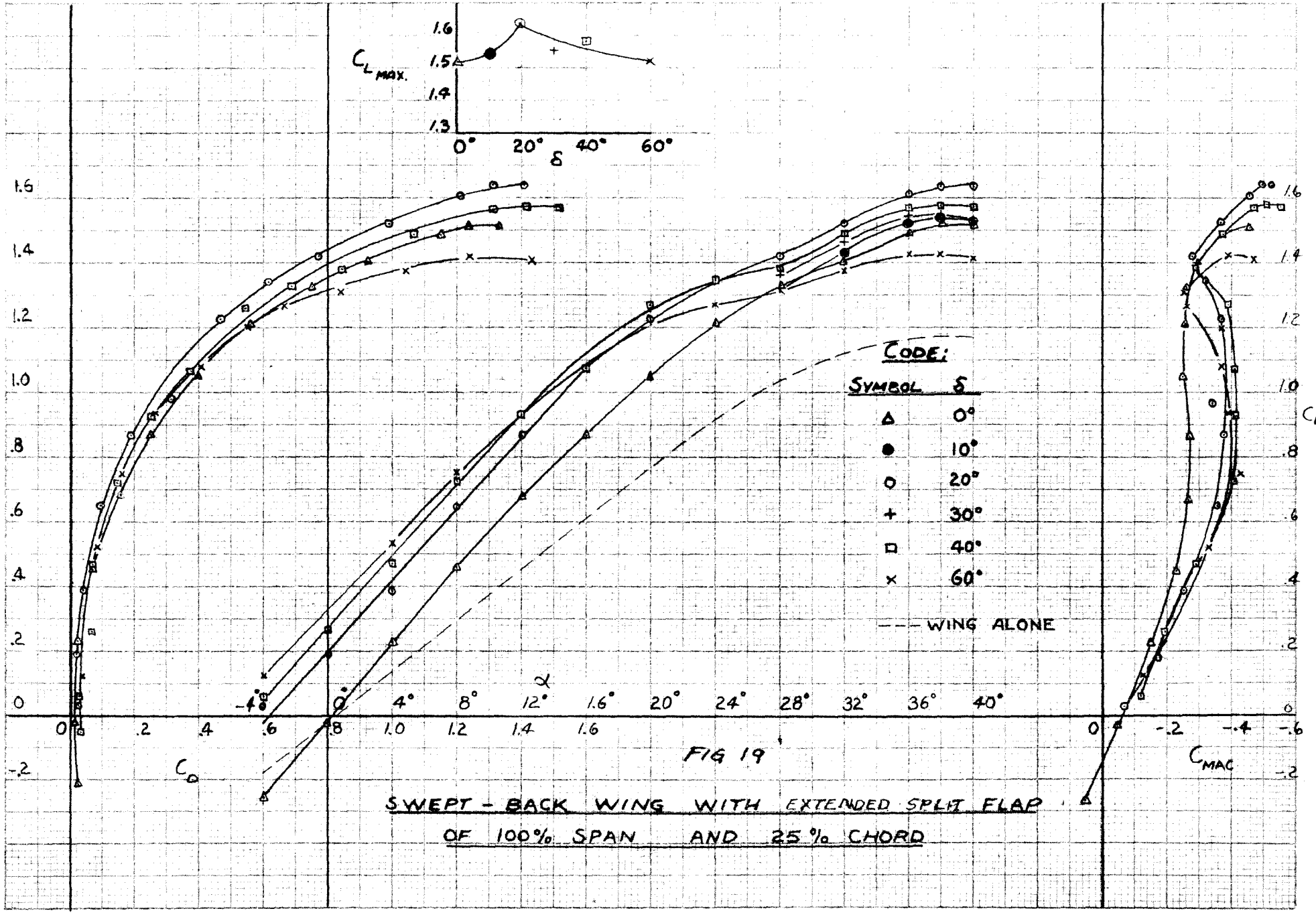

FIG 19

SWEPT - BACK WING WITH EXTENDED SPLIT FLAP OF 100% SPAN AND 25% CHORD

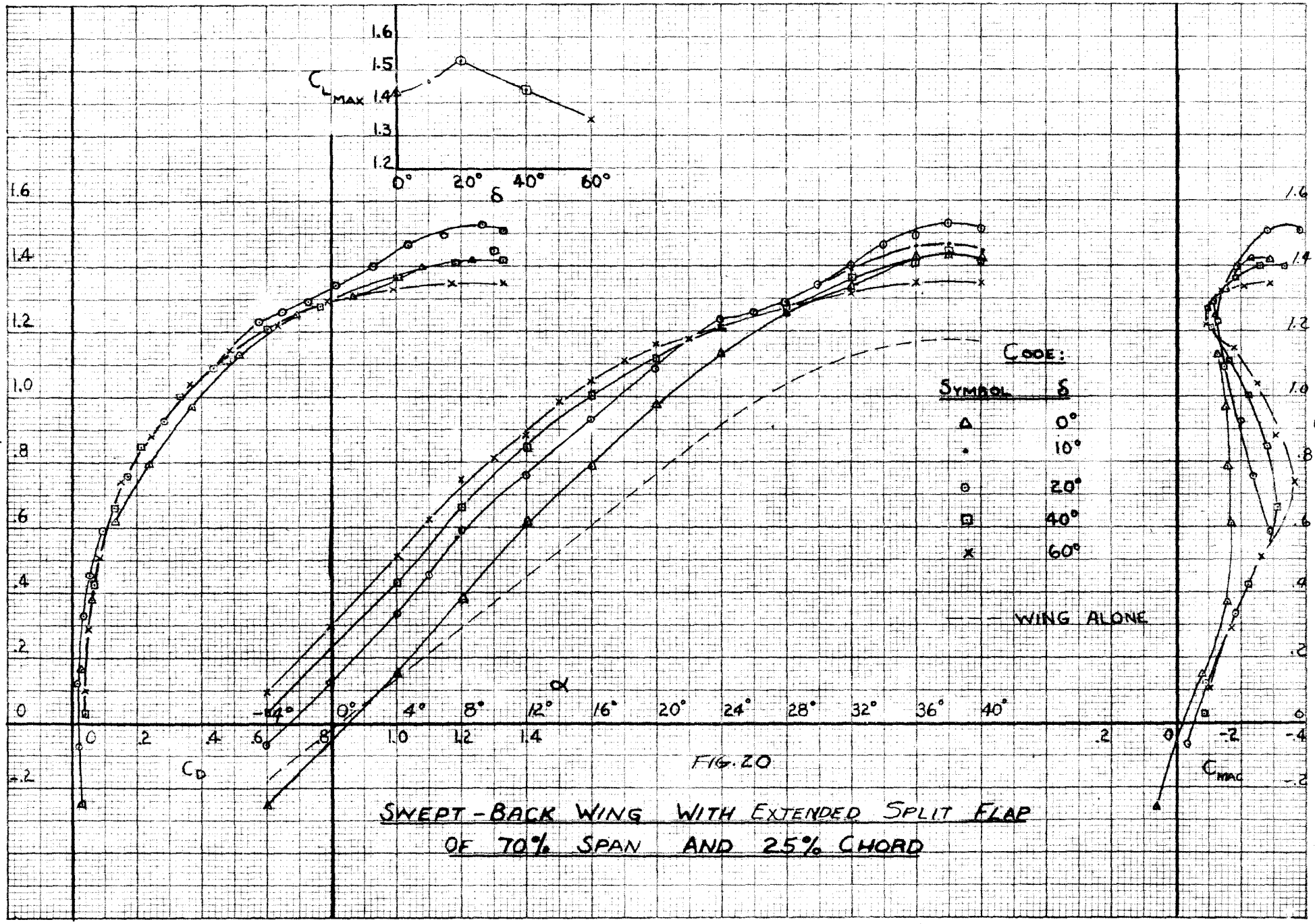

FIG. 20

SWEPT-BACK WING WITH EXTENDED SPLIT FLAP OF 70% SPAN AND 25% CHORD

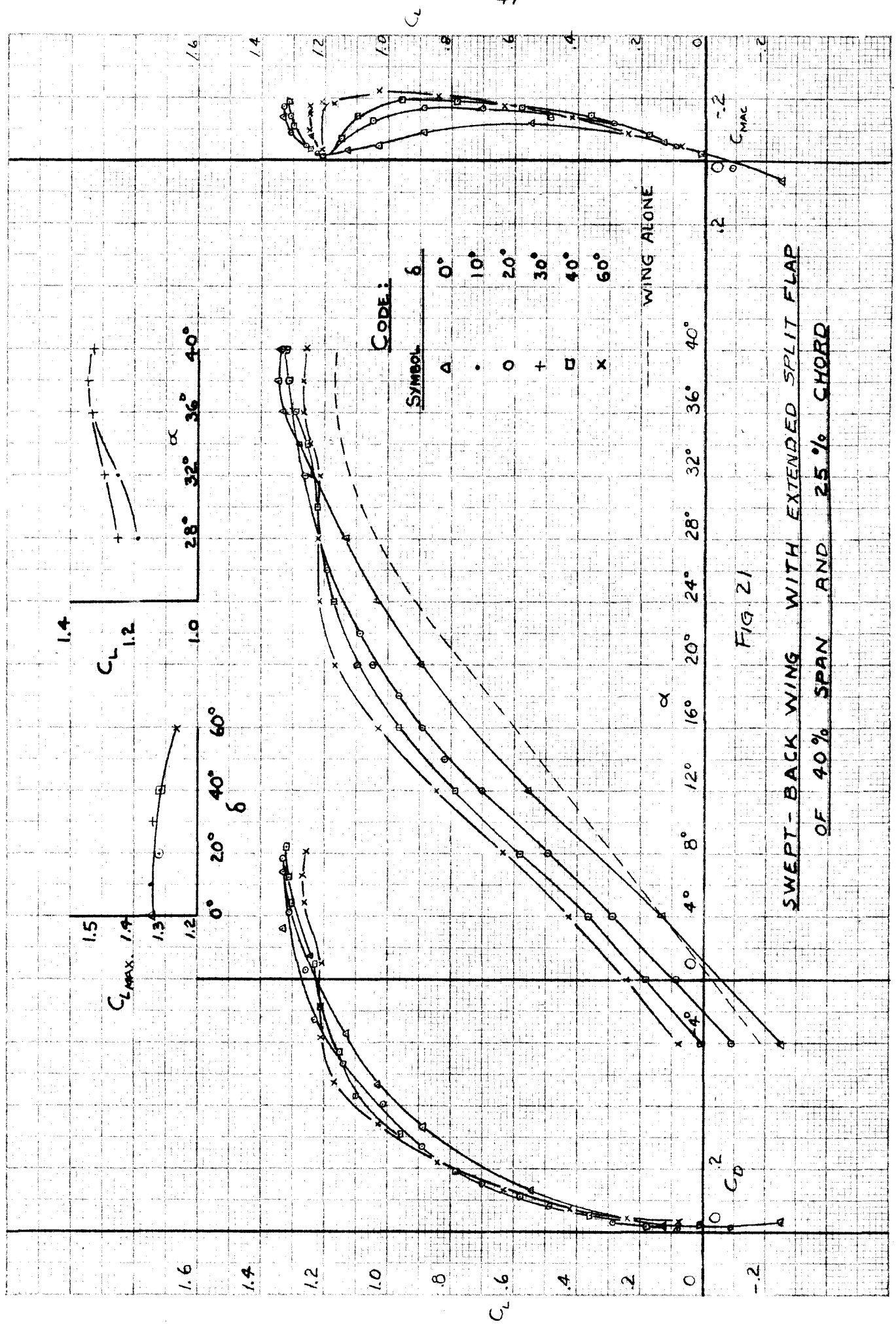
SWEPT-BACK WING WITH EXTENDED SPLIT FLAP
OF 40% SPAN AND 25% CHORD
FIG 21
WING ALONE
CODE:
SYMBOL δ
0°
10°
20°
30°
40°
60°
α
C_L
C_D
C_{MAC}
$C_{L_{MAX.}}$
δ

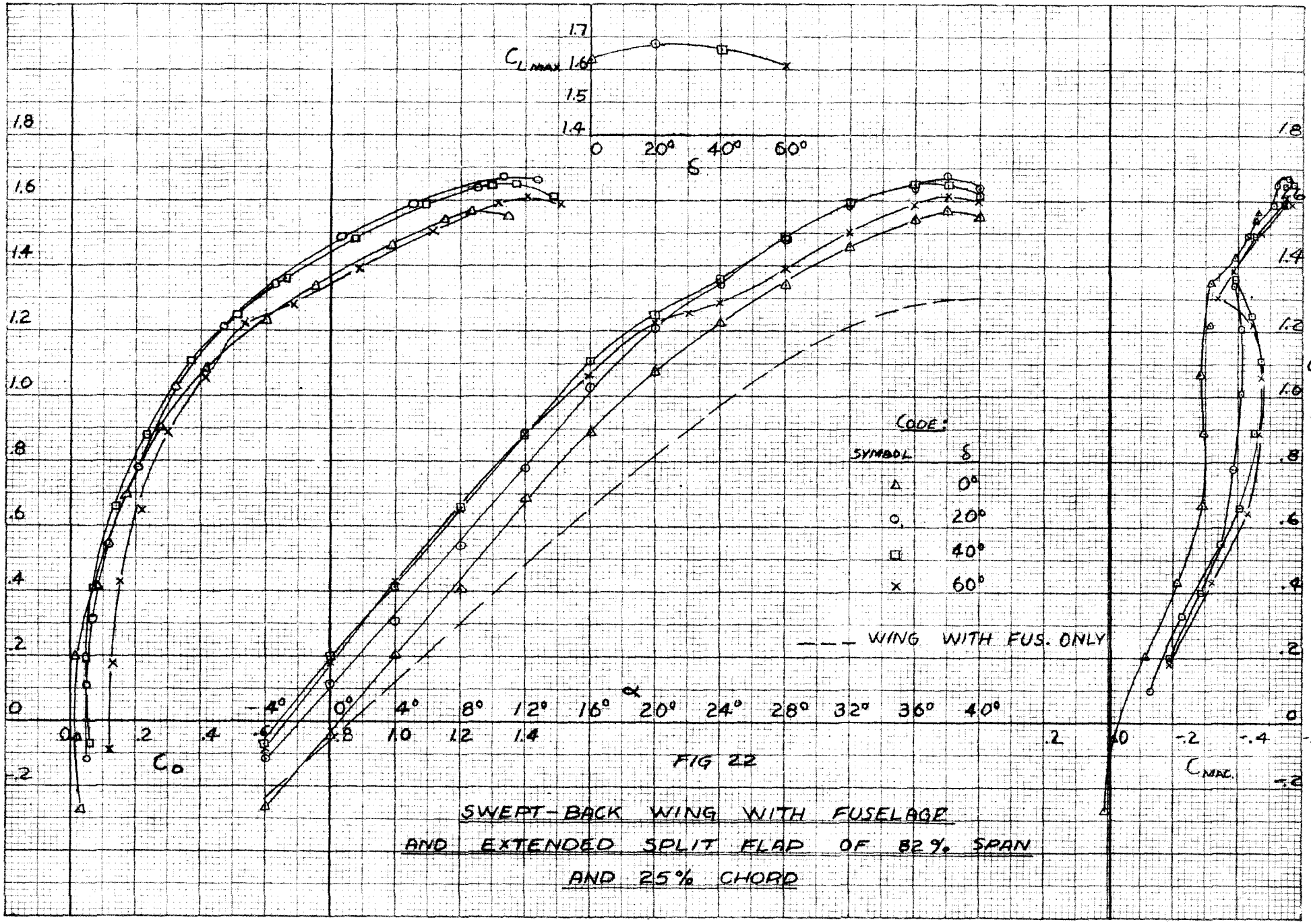

FIG 22

SWEPT-BACK WING WITH FUSELAGE AND EXTENDED SPLIT FLAP OF 82% SPAN AND 25% CHORD

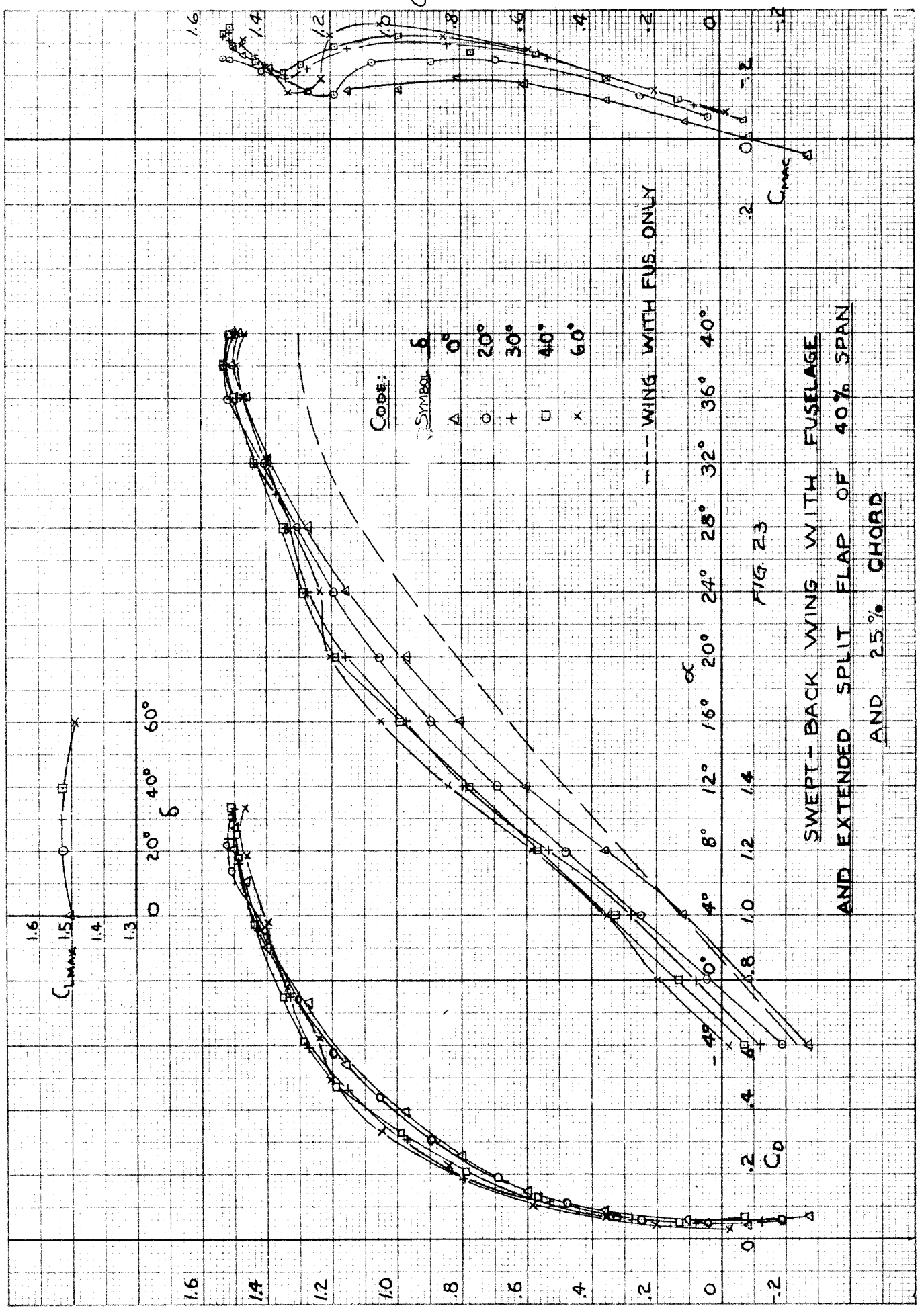

FIG 23

SWEPT-BACK WING WITH FUSELAGE
AND EXTENDED SPLIT FLAP OF 40% SPAN
AND 25% CHORD

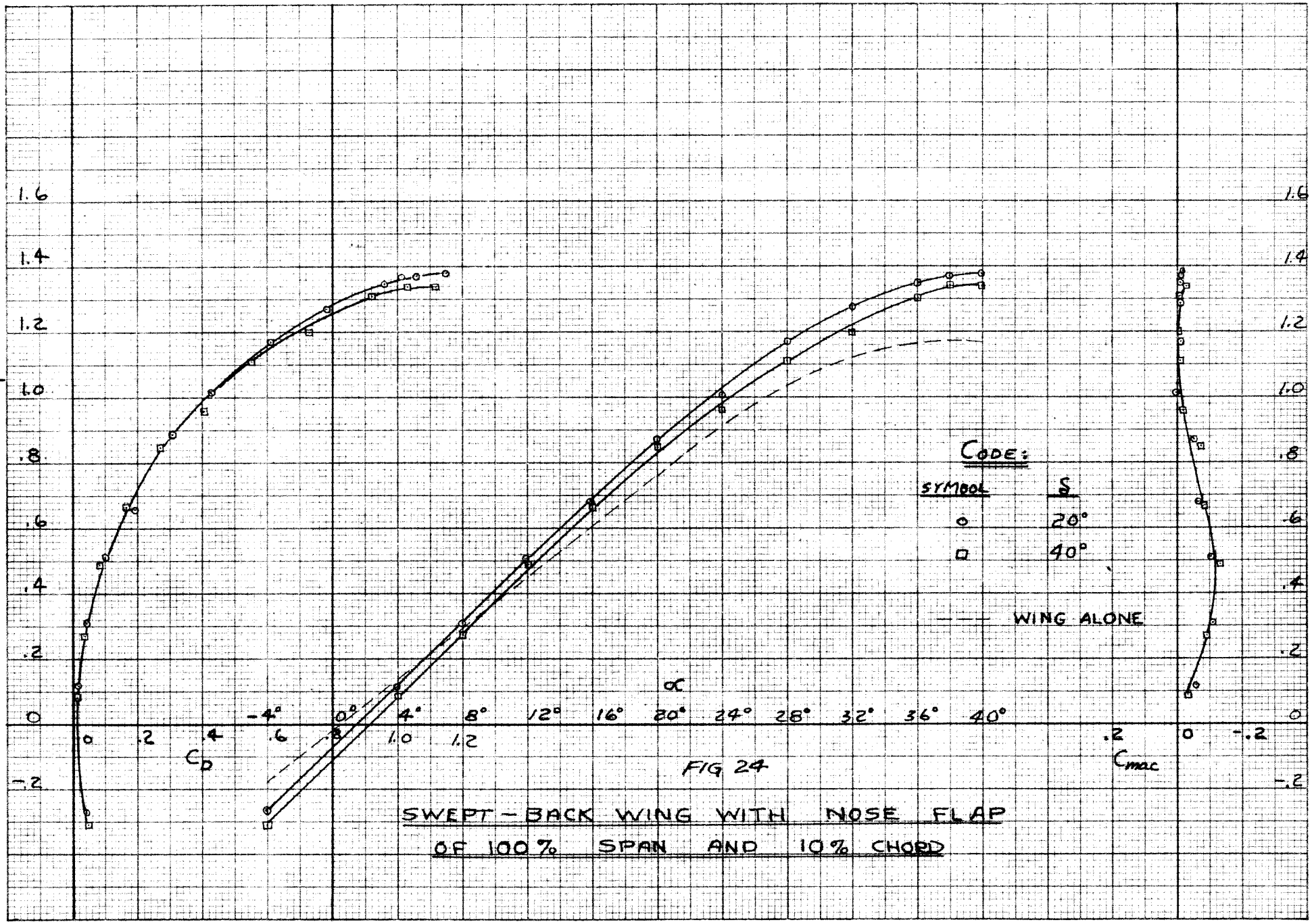

FIG 24

SWEPT-BACK WING WITH NOSE FLAP OF 100% SPAN AND 10% CHORD

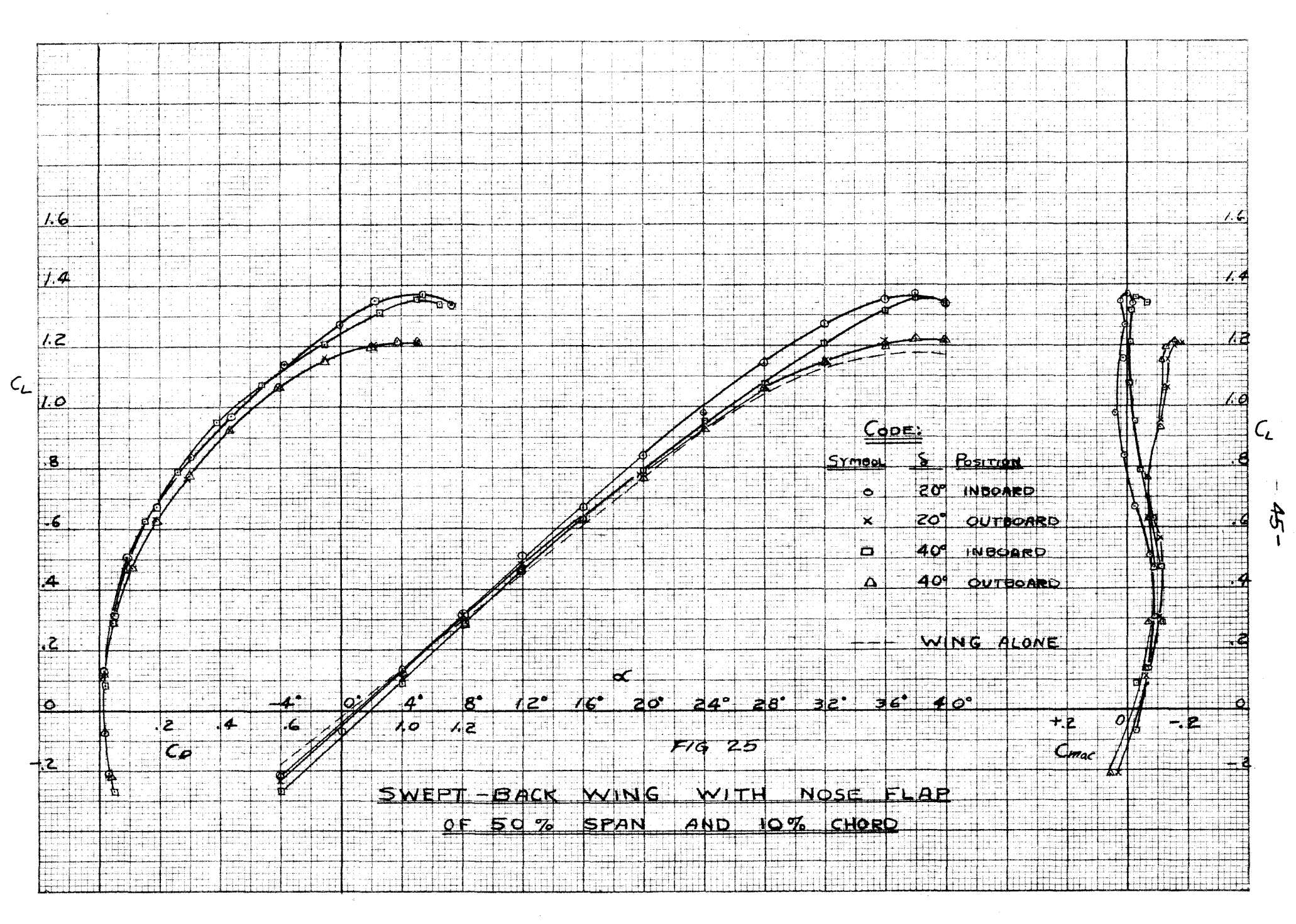

FIG 25

SWEPT-BACK WING WITH NOSE FLAP
OF 50% SPAN AND 10% CHORD

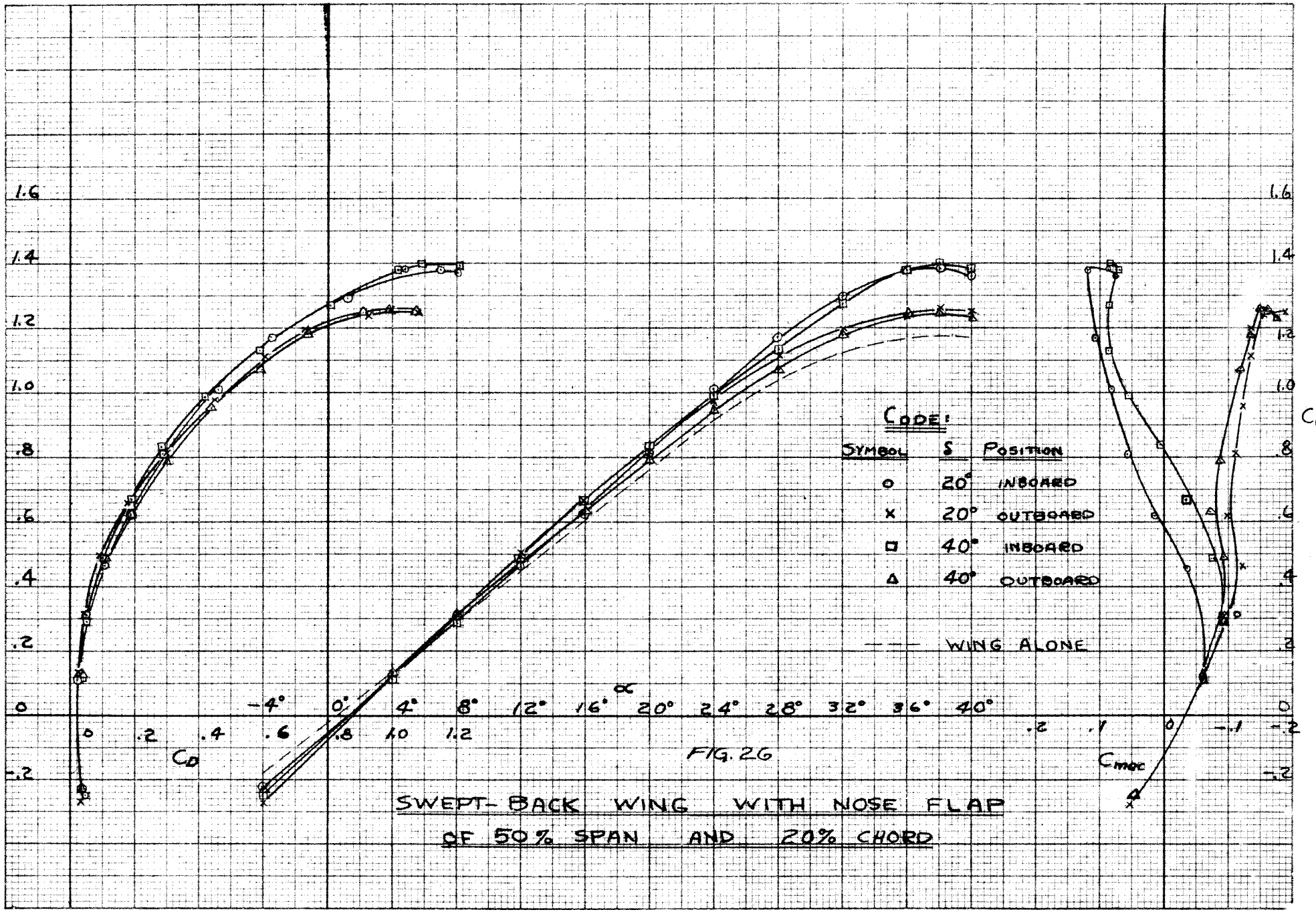

FIG. 26

SWEPT-BACK WING WITH NOSE FLAP OF 50% SPAN AND 20% CHORD

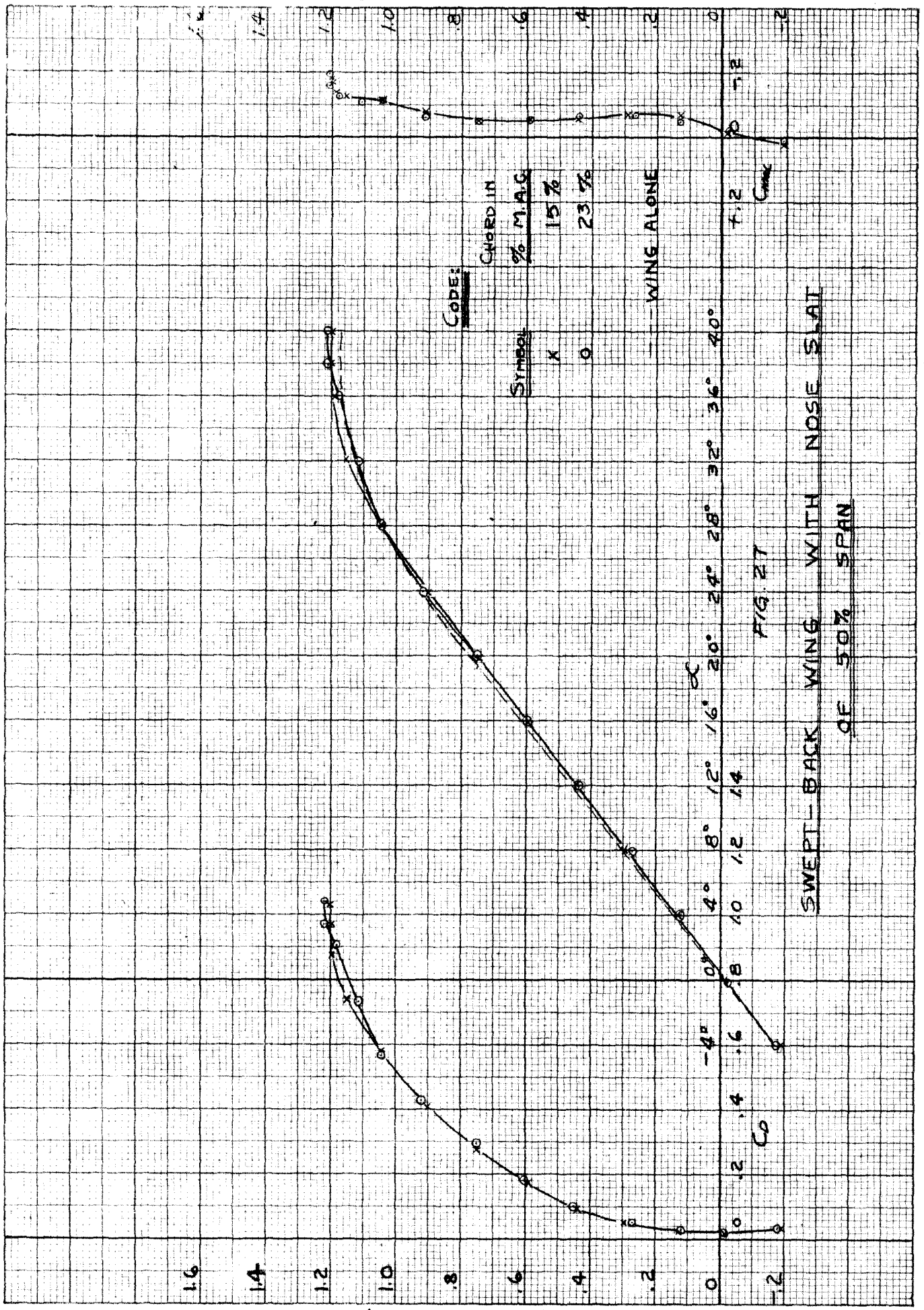

FIG 27

SWEPT-BACK WING WITH NOSE SLAT OF 50% SPAN

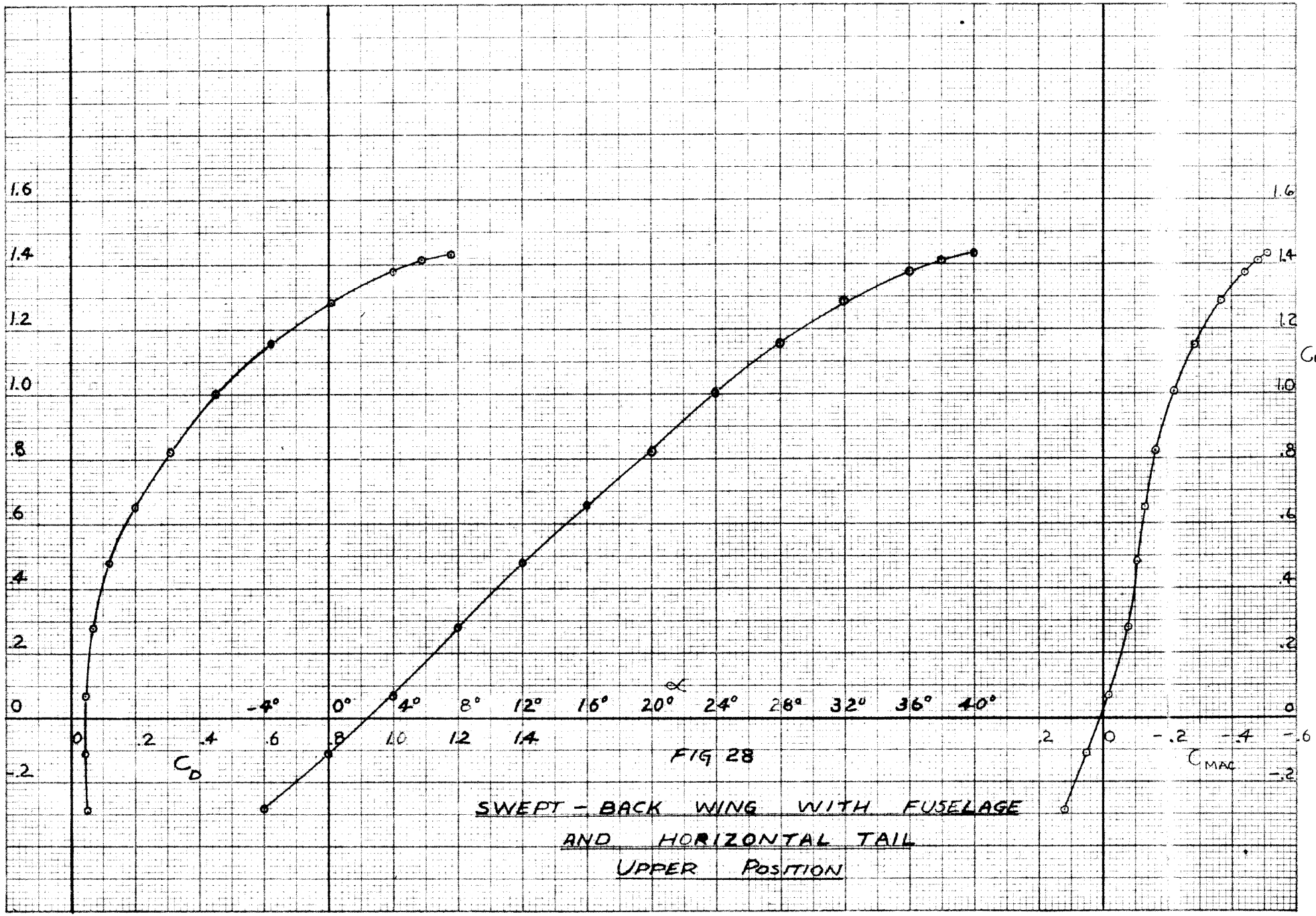

FIG 28

SWEPT - BACK WING WITH FUSELAGE AND HORIZONTAL TAIL UPPER POSITION

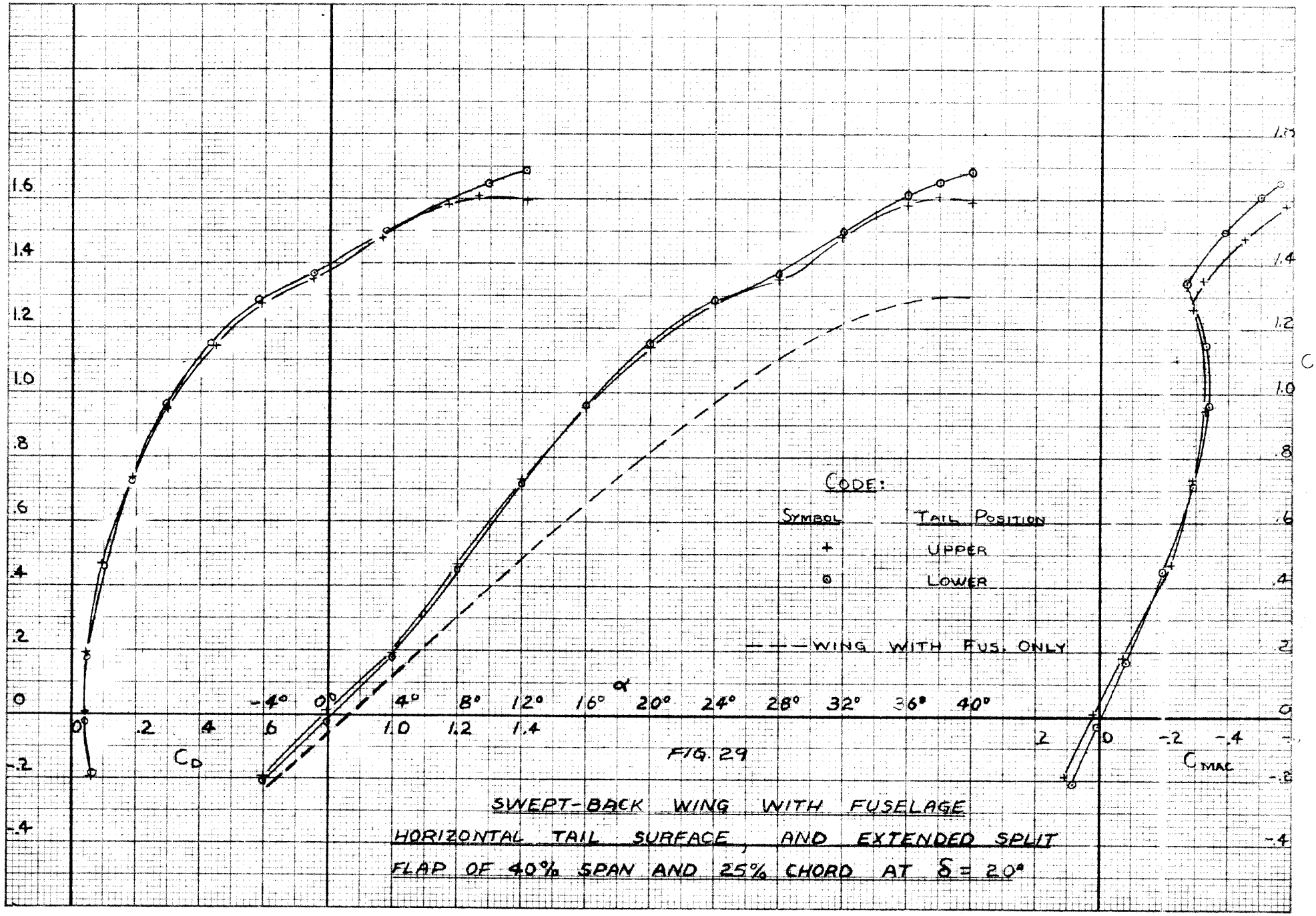

FIG. 29

SWEPT-BACK WING WITH FUSELAGE HORIZONTAL TAIL SURFACE, AND EXTENDED SPLIT FLAP OF 40% SPAN AND 25% CHORD AT $\delta = 20°$

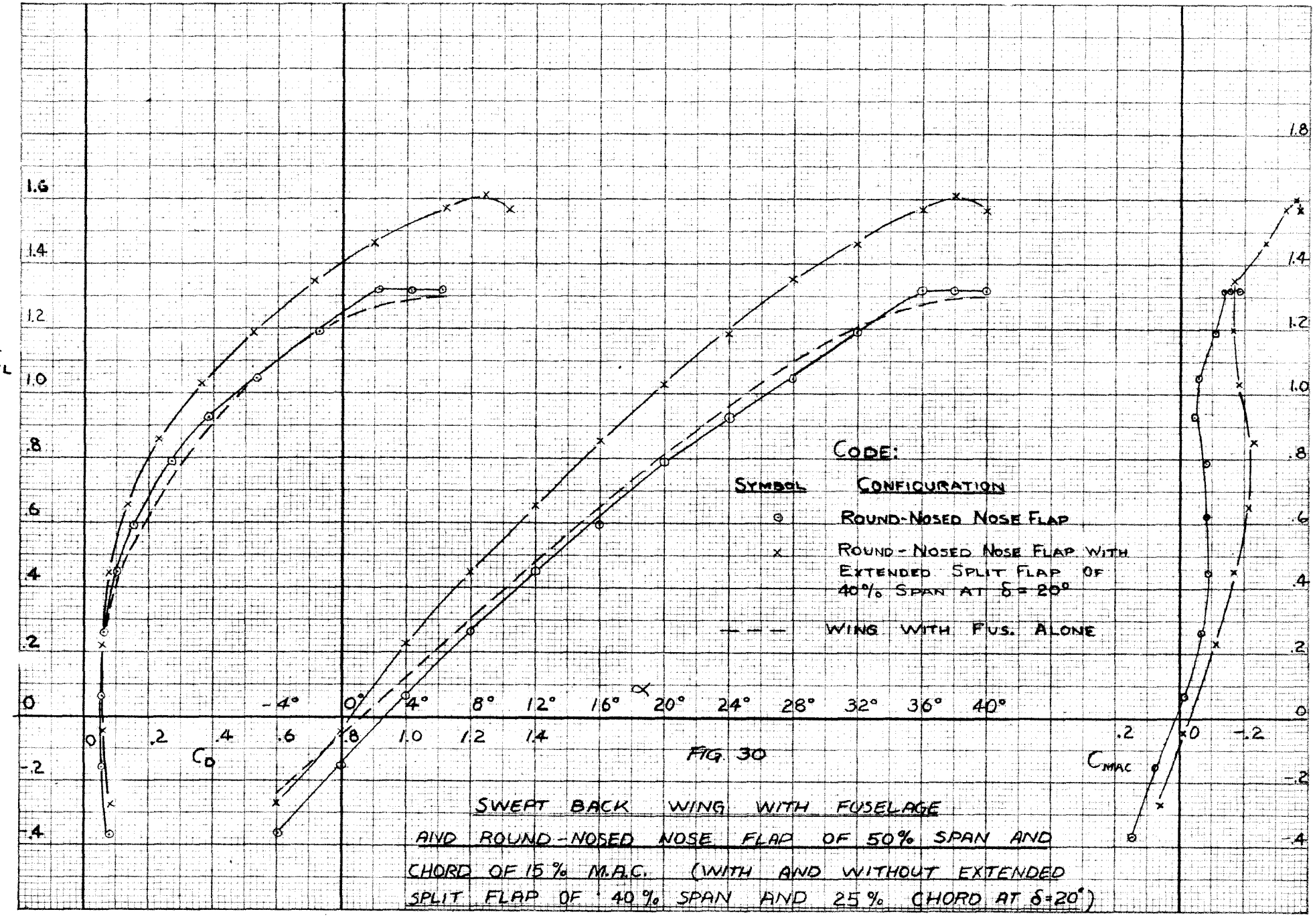

FIG. 30

SWEPT BACK WING WITH FUSELAGE AND ROUND-NOSED NOSE FLAP OF 50% SPAN AND CHORD OF 15% M.A.C. (WITH AND WITHOUT EXTENDED SPLIT FLAP OF 40% SPAN AND 25% CHORD AT δ=20°)

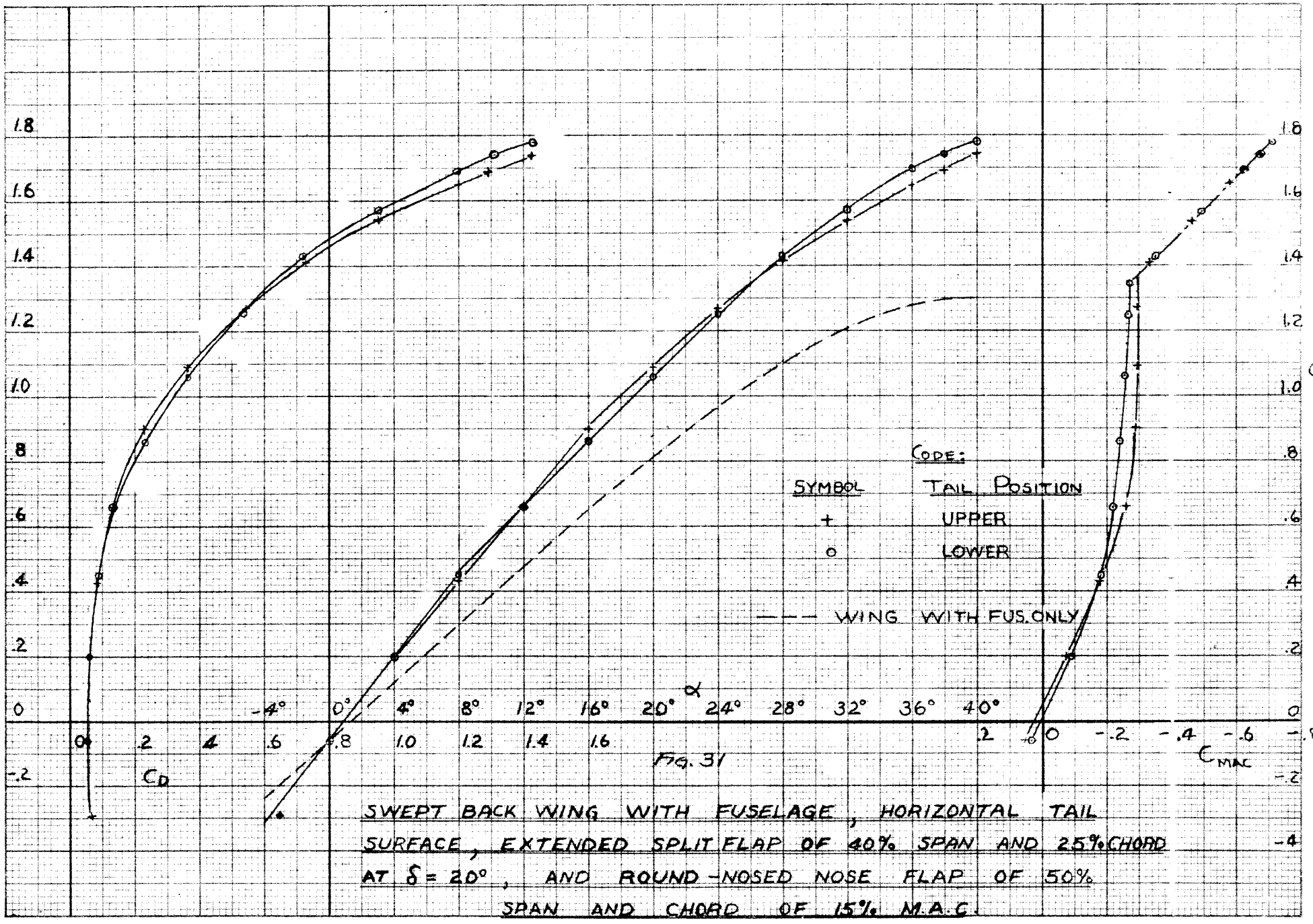

Fig. 31

SWEPT BACK WING WITH FUSELAGE, HORIZONTAL TAIL SURFACE, EXTENDED SPLIT FLAP OF 40% SPAN AND 25% CHORD AT $\delta = 20°$, AND ROUND-NOSED NOSE FLAP OF 50% SPAN AND CHORD OF 15% M.A.C.

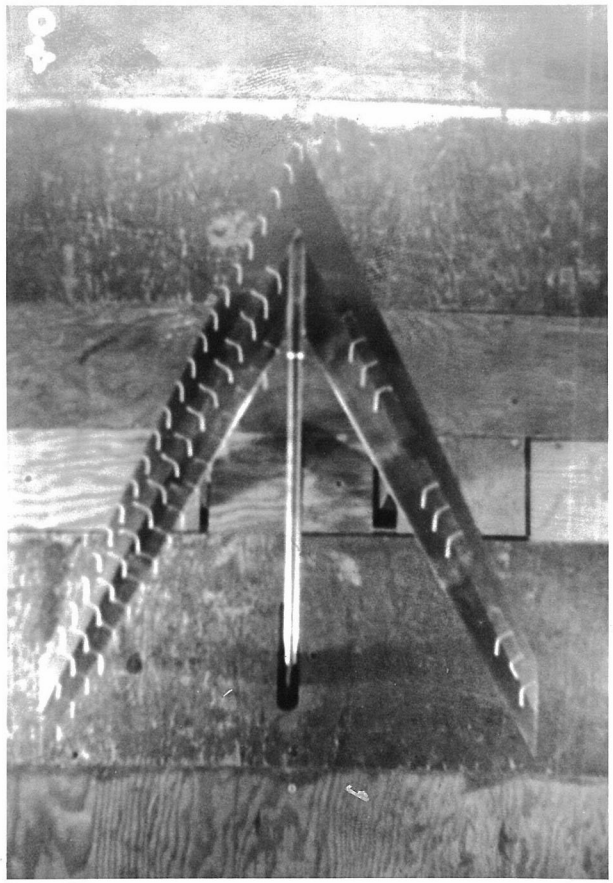

$\alpha = 0°$

Fig. 32

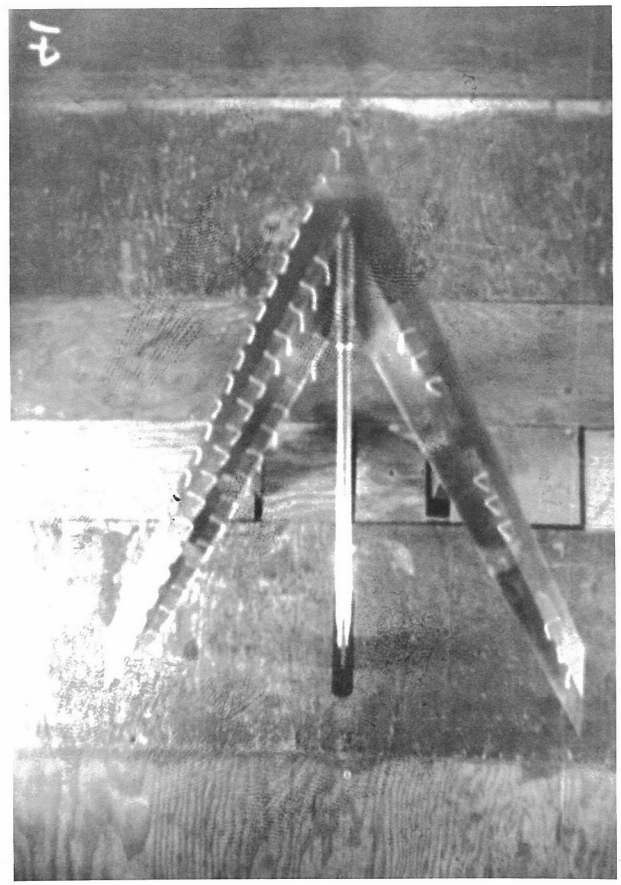

$\alpha = 8°$

Fig. 33

Tuft Studies of Wing With 70% Span

Split Flap Deflected 20°

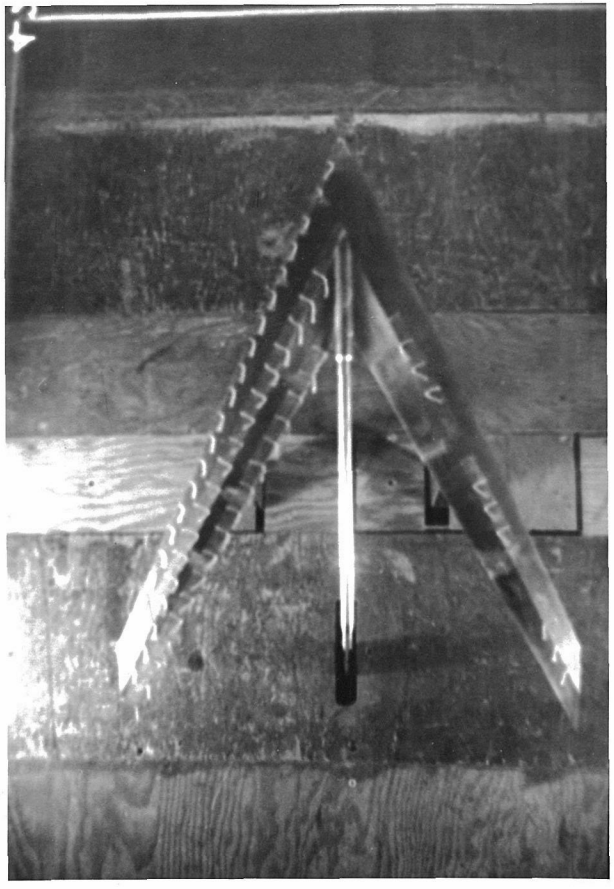

$\alpha = 12°$

Fig. 34

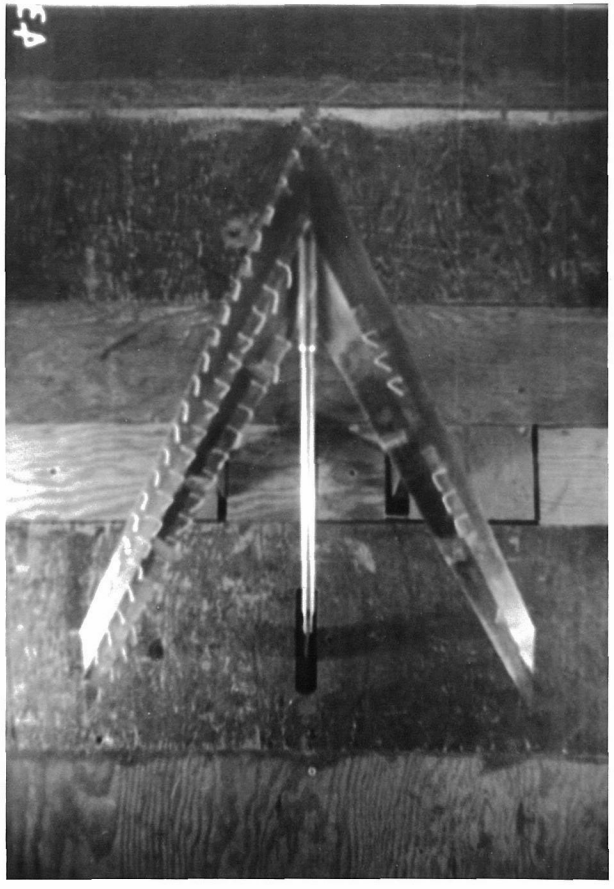

$\alpha = 16°$

Fig. 35

Tuft Studies of Wing With 70% Span

Split Flap Deflected 20°

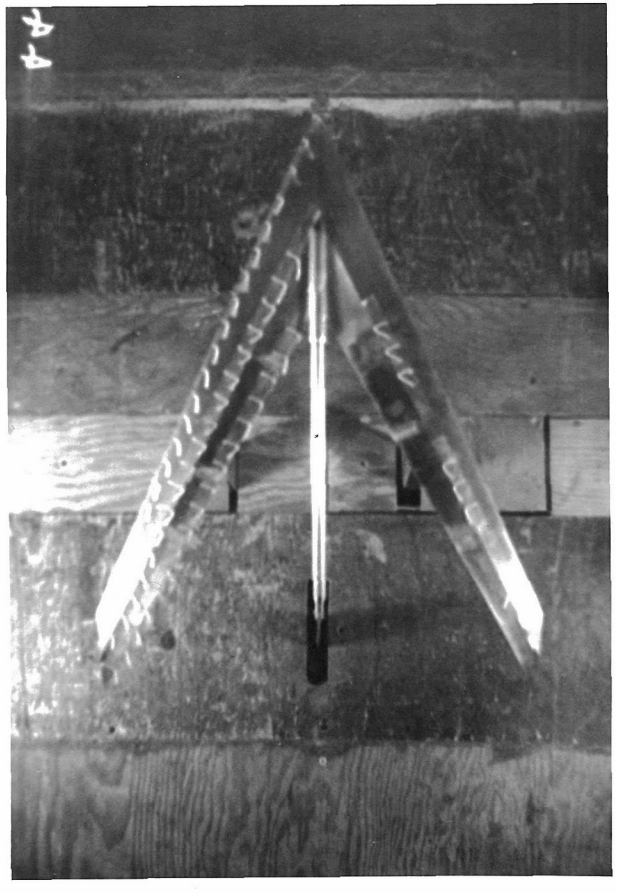

$\alpha = 20°$

Fig. 36

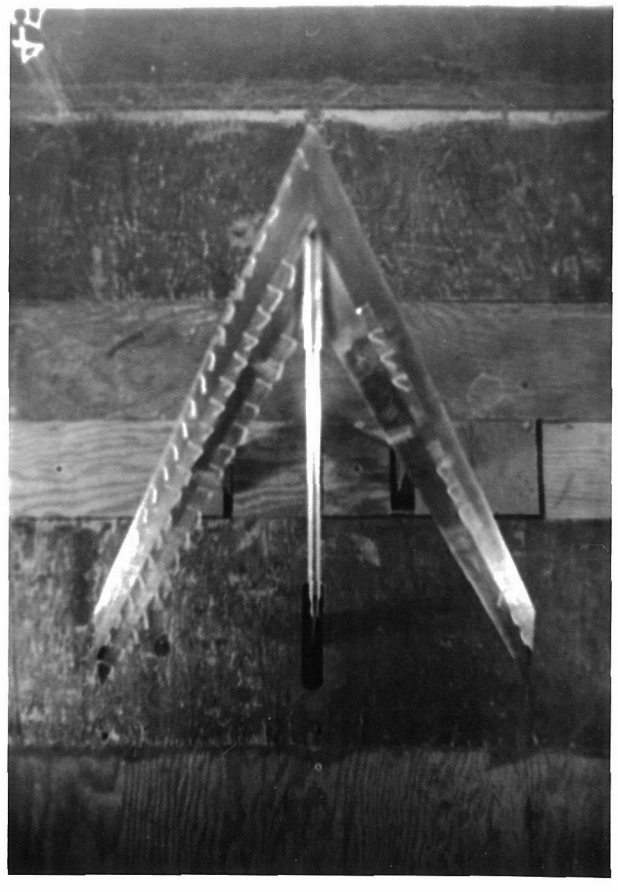

$\alpha = 24°$

Fig. 37

Tuft Studies of Wing With 70% Span

Split Flap Deflected 20°

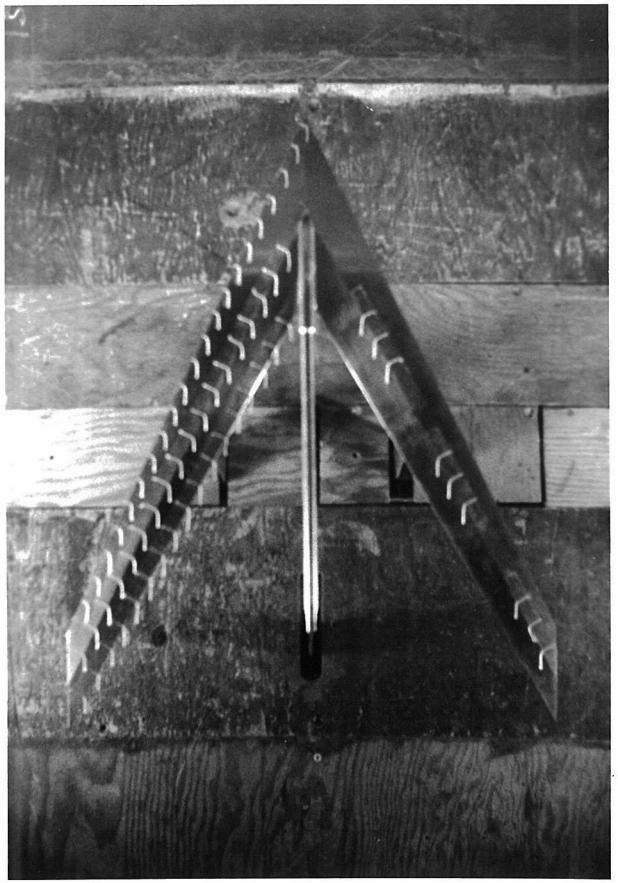

$\alpha = 0°$

Fig. 38

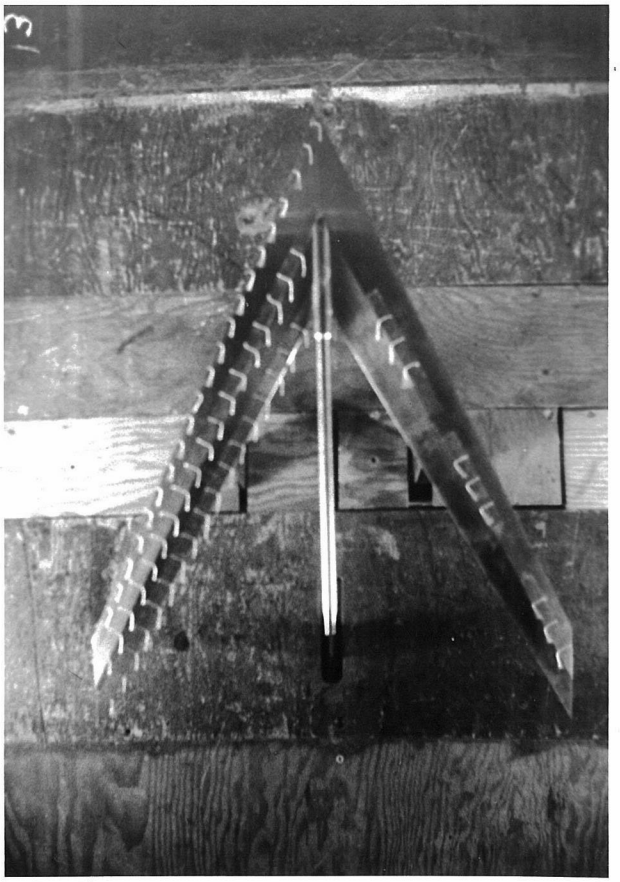

$\alpha = 4°$

Fig. 39

Tuft Studies of Wing Alone

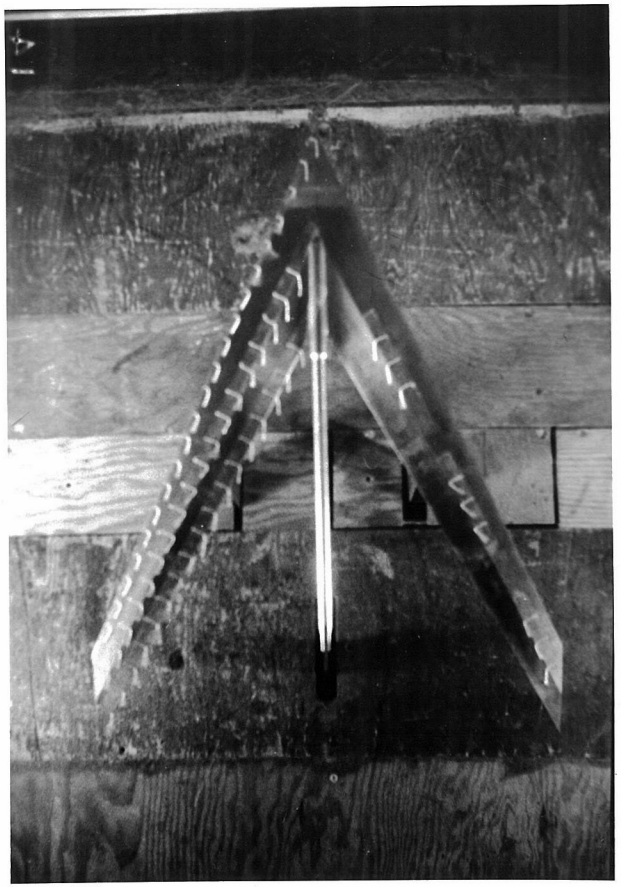

$\alpha = 8°$

Fig. 40

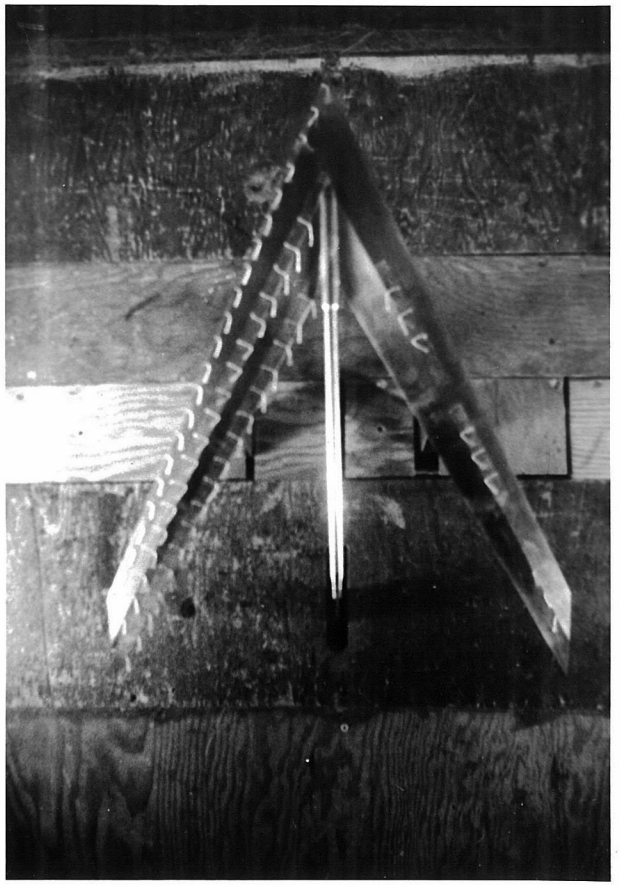

$\alpha = 12°$

Fig. 41

Tuft Studies of Wing Alone

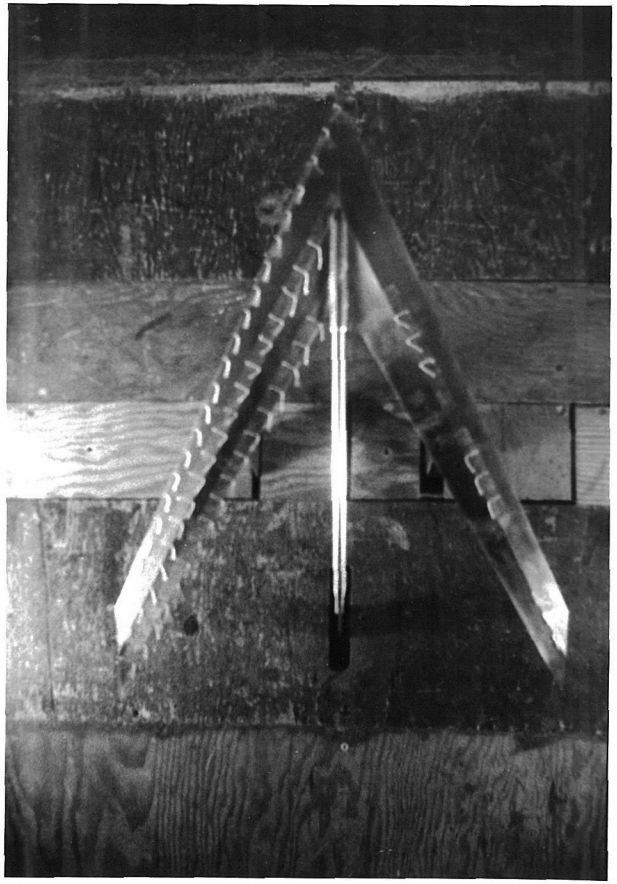

$\alpha = 16°$

Fig. 42

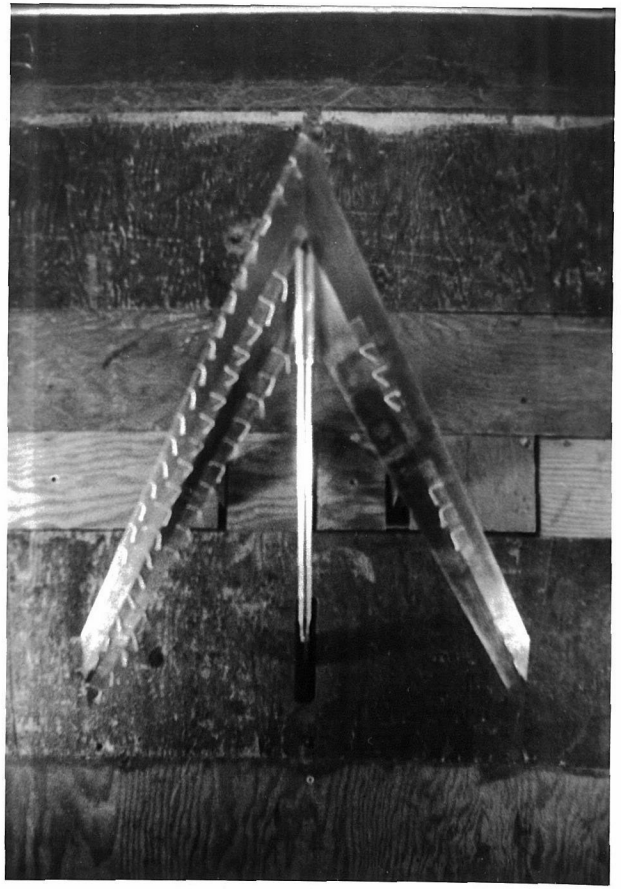

$\alpha = 20°$

Fig. 43

Tuft Studies of Wing Alone

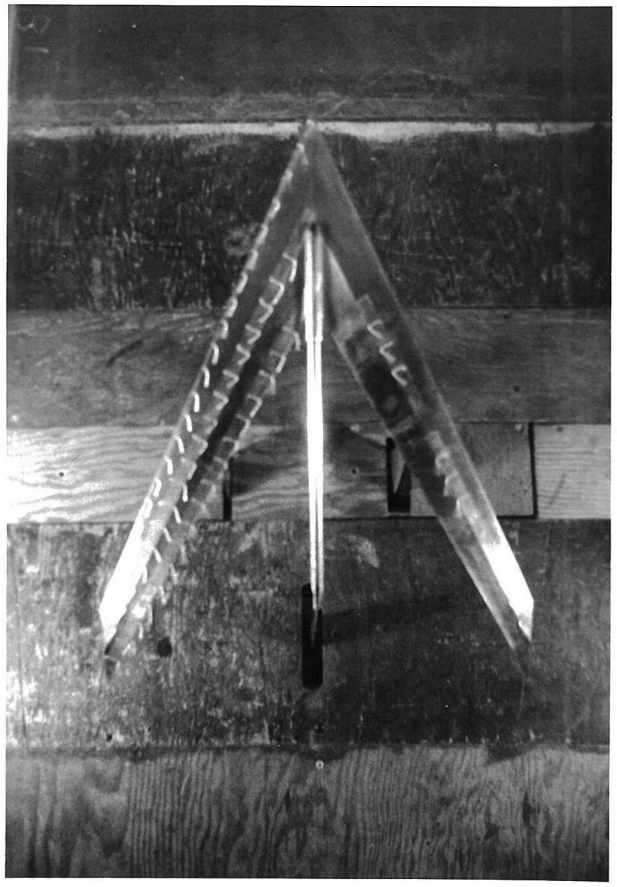

$\alpha = 24°$

Fig. 44

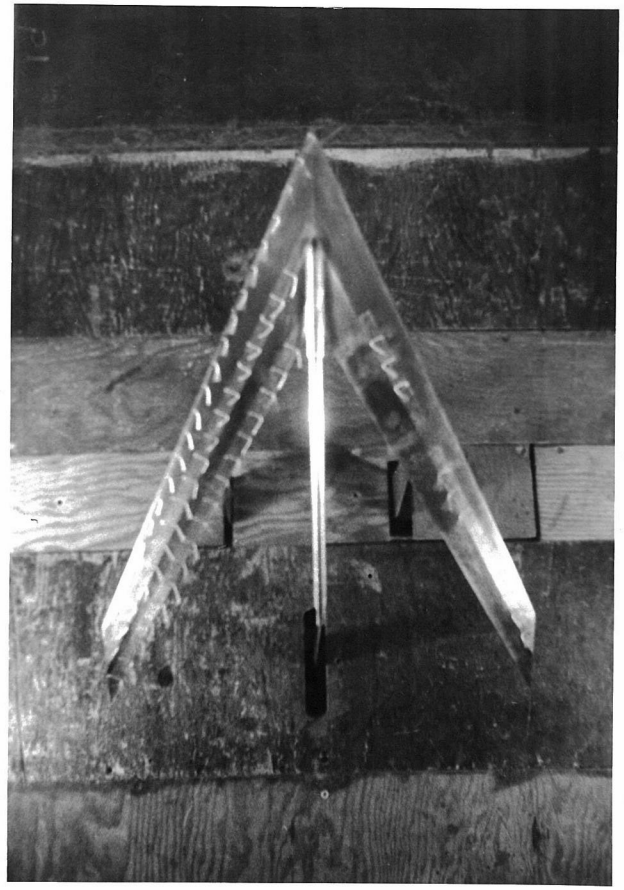

$\alpha = 28°$

Fig. 45

Tuft Studies of Wing Alone

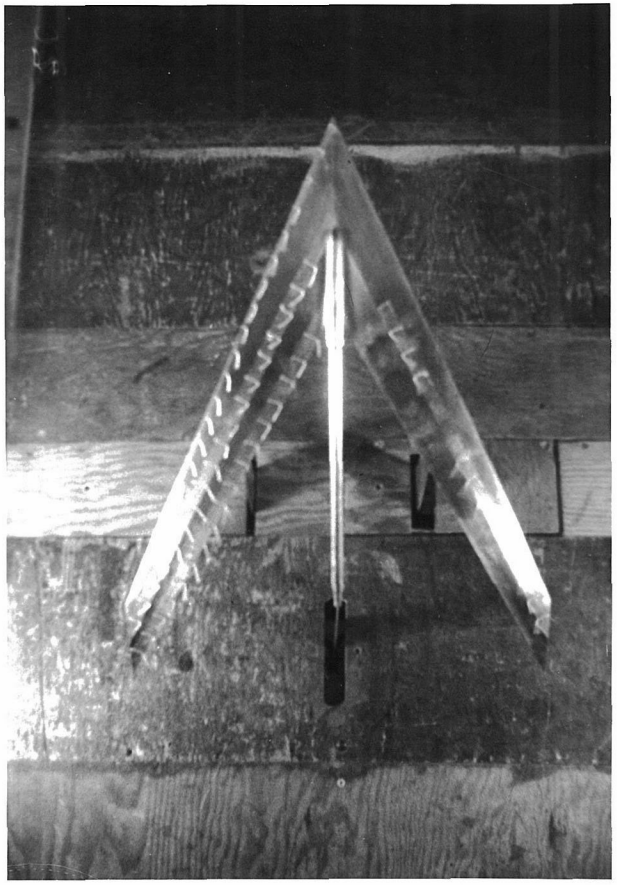

$\alpha = 32°$

Fig. 46

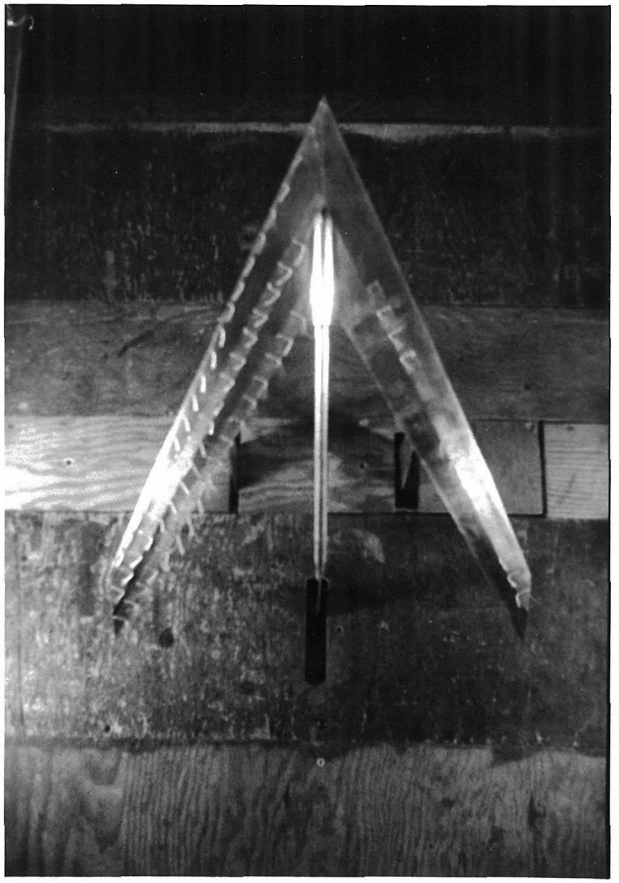

$\alpha = 36°$

Fig. 47

Tuft Studies of Wing Alone

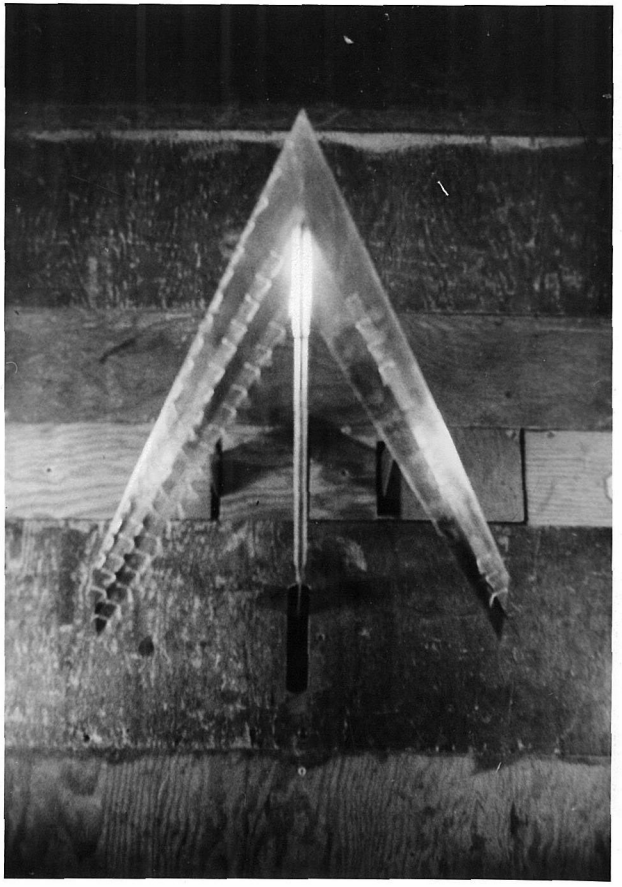

$\alpha = 40°$

Fig. 48

Tuft Studies of Wing Alone